



Cross-helicity effect on α -type dynamo in non-equilibrium turbulence

Krzysztof A. Mizerski ^{1,†}, Nobumitsu Yokoi ^{1,2} and
Axel Brandenburg ^{1,3,4,5,6}

¹Department of Magnetism, Institute of Geophysics, Polish Academy of Sciences, Ksiecia Janusza 64,
01-452 Warsaw, Poland

²Institute of Industrial Science, University of Tokyo, Komaba, Meguro, Tokyo 153-8505, Japan

³Nordita, KTH Royal Institute of Technology and Stockholm University, Hannes Alfvéns väg 12, 10691
Stockholm, Sweden

⁴The Oskar Klein Centre, Department of Astronomy, Stockholm University, AlbaNova, 10691 Stockholm,
Sweden

⁵School of Natural Sciences and Medicine, Ilia State University, 0194 Tbilisi, Georgia

⁶McWilliams Center for Cosmology and Department of Physics, Carnegie Mellon University, Pittsburgh,
PA 15213, USA

(Received 2 March 2023; revised 29 May 2023; accepted 31 May 2023)

Turbulence is typically not in equilibrium, i.e. mean quantities such as the mean energy and helicity are typically time-dependent. The effect of non-stationarity on the turbulent hydromagnetic dynamo process is studied here with the use of the two-scale direct-interaction approximation, which allows one to explicitly relate the mean turbulent Reynolds and Maxwell stresses and the mean electromotive force to the spectral characteristics of turbulence, such as the mean energy, as well as kinetic and cross-helicity. It is demonstrated that the non-equilibrium effects can enhance the dynamo process when the magnetohydrodynamic turbulence is both helical and cross-helical. This effect is based on the turbulent infinitesimal-impulse cross-response functions, which do not affect turbulent flows in equilibrium. The evolution and sources of the cross-helicity in magnetohydrodynamic turbulence are also discussed.

Key words: astrophysical plasmas, plasma dynamics, plasma nonlinear phenomena

1. Introduction

The effect of hydromagnetic dynamo action is ubiquitous in astrophysical plasmas, e.g. in stellar and planetary interiors, accretion discs or the interstellar medium (Roberts & Soward 1972; Balbus & Hawley 1991a,b; Brandenburg & Subramanian 2005; Dormy & Soward 2007; Roberts & King 2013). This is particularly important in view of the recent advancement of tokamak devices, reaching very high plasma temperatures, thus giving hope for the production of thermonuclear fusion power (Li, Ni & Lu 2019; Gibney 2022). The investigation of the large-scale dynamo mechanisms in magnetohydrodynamic

† Email address for correspondence: kamiz@igf.edu.pl

(MHD) turbulence, that is, those that lead to generation of large-scale magnetic fields, is mainly limited to equilibrium, i.e. statistically stationary turbulence.

One of the widely known and often invoked dynamo mechanisms is the so-called α -effect, which requires chirality (lack of reflectional symmetry) in turbulent flow, and this requires some mechanism that breaks the ‘up–down’ symmetry of the system (Krause & Rädler 1980; Dormy & Soward 2007; Moffatt & Dormy 2019). A large-scale electromotive force (EMF) is then generated and this leads to the amplification of magnetic energy. The lack of reflectional symmetry is typically introduced by stratification and background rotation and a useful measure of the flow chirality is the kinetic helicity. Another pseudoscalar quantity of importance in dynamo theory is the cross-helicity (e.g. Hamba & Tsuchiya 2010; Yokoi 2013; see Yokoi (2023b) for a review).

The aim of this paper can be shortly stated as a demonstration of the influence of non-equilibrium effects in MHD turbulence on the α -effect and thereby on large-scale dynamos. This issue has already been investigated in a series of papers by Mizerski (2018a,b, 2020, 2021a, 2022), which, however, assumed that the turbulence was stirred by a Gaussian and helical forcing; the physical properties of the forcing were then present in the expressions for the α coefficient. It has been shown that the α -effect can be induced by interactions between waves with distinct but close frequencies (thus the term ‘beating’ waves, which induce non-stationarity), leading to a finite magnetic field amplification rate independent of the magnetic diffusivity η , that is, operating even in the limit of vanishing fluid resistivity. Such an α -effect is proportional to the energy production rate in non-stationary turbulence and the non-equilibrium effects play a more significant role when the magnetic diffusivity is weak, $\eta \ll \nu$. Furthermore, in Mizerski (2021a) the effect of non-stationarity was shown to induce an out-of-phase slow temporal evolution of the turbulent coefficient α and the turbulent diffusivity β , implying the existence of periods of enhanced and suppressed turbulent dynamo processes. In particular, the enhancement of diffusion sometimes coincides with the suppression of the α -effect, leading to magnetic field decay, i.e. a field excursion. In Mizerski (2022) the non-equilibrium effects in the interstellar medium driven by supernova ejections and the difference between the ejection rates for type I and type II supernovae, based on a simple theoretical model, have been argued to provide a significant contribution to the mean EMF. The non-equilibrium dynamo mechanisms may shed some light on the issue of large-scale magnetic field generation in highly conducting plasmas. It is of interest to mention that in the recent numerical simulations of Zhou & Blackman (2023), an η -independent large-scale dynamo regime was identified in the setting of a $(2\pi)^3$ -periodic box, confirming that at high magnetic Reynolds numbers large-scale dynamo mechanisms still persist.

Here, on the other hand, we apply the two-scale direct-interaction approximation (TSDIA), which allows us to remove the stirring force, but instead we need to assume some statistical properties of the background turbulence. Nevertheless, this approach allows one to explicitly relate the mean EMF to kinetic helicity and cross-helicity, through consideration of Green’s response functions, which describe the responses of the turbulent flow and magnetic field to infinitesimal perturbations (see e.g. Yoshizawa 1985, 1990, 1998; Yokoi 2013, 2018). We show that the infinitesimal-impulse cross-responses affect the mean EMF through non-equilibrium effects in MHD turbulence, and the α -effect is potentially enhanced, provided that the kinetic helicity and cross-helicity are both non-zero. We also discuss the evolution equation of the cross-helicity, its sources and sinks in MHD turbulence, and hence the possibility of a coexistence of the kinetic helicity and cross-helicity; this issue is also investigated numerically.

2. Mathematical formulation

To study the MHD turbulence in an incompressible conducting fluid we consider the following dynamical equations describing the evolution of the velocity field of the fluid flow $\mathbf{U}(\mathbf{x}, t)$ and the magnetic field $\mathbf{B}(\mathbf{x}, t)$:

$$\frac{\partial \mathbf{U}}{\partial t} + (\mathbf{U} \cdot \nabla) \mathbf{U} = -\nabla \Pi - 2\boldsymbol{\Omega} \times \mathbf{U} + (\mathbf{B} \cdot \nabla) \mathbf{B} + \nu \nabla^2 \mathbf{U}, \quad (2.1a)$$

$$\frac{\partial \mathbf{B}}{\partial t} + (\mathbf{U} \cdot \nabla) \mathbf{B} = (\mathbf{B} \cdot \nabla) \mathbf{U} + \eta \nabla^2 \mathbf{B}, \quad (2.1b)$$

$$\nabla \cdot \mathbf{U} = 0 \quad \nabla \cdot \mathbf{B} = 0, \quad (2.1c)$$

where

$$\Pi = \frac{p}{\rho} + \frac{\mathbf{B}^2}{2} - \frac{1}{2}(\boldsymbol{\Omega} \times \mathbf{x})^2 \quad (2.2)$$

is the total pressure, ρ is the density, $\boldsymbol{\Omega}$ is the angular velocity, ν is the viscosity and η is the magnetic diffusivity. For the purpose of simplicity we rescaled the magnetic field in the following way: $\mathbf{B}/\sqrt{\mu_0\rho} \rightarrow \mathbf{B}$, where μ_0 is the vacuum permeability (so that the prefactor $1/\mu_0\rho$ in the Lorentz force term in the Navier–Stokes equation is lost); in the following we also rescale the currents, $\sqrt{\mu_0/\rho}\mathbf{J} \rightarrow \mathbf{J}$, so that $\mathbf{J} = \nabla \times \mathbf{B}$. Next, denoting by angular brackets the ensemble mean,

$$\langle \cdot \rangle \text{ -- ensemble mean,} \quad (2.3)$$

we put forward the standard decomposition

$$\mathbf{U} = \langle \mathbf{U} \rangle + \mathbf{u}', \quad \mathbf{B} = \langle \mathbf{B} \rangle + \mathbf{b}', \quad p = \langle p \rangle + p', \quad (2.4a-c)$$

and write down separately the equations for the mean fields $\langle \mathbf{U} \rangle$ and $\langle \mathbf{B} \rangle$ and the turbulent fluctuations \mathbf{u}' and \mathbf{b}' ; this yields

$$\begin{aligned} \frac{\partial \langle \mathbf{U} \rangle}{\partial t} + ((\langle \mathbf{U} \rangle \cdot \nabla) \langle \mathbf{U} \rangle) &= -\nabla \langle \Pi \rangle - 2\boldsymbol{\Omega} \times \langle \mathbf{U} \rangle + ((\langle \mathbf{B} \rangle \cdot \nabla) \langle \mathbf{B} \rangle + \nu \nabla^2 \langle \mathbf{U} \rangle \\ &\quad - \nabla \cdot (\langle \mathbf{u}' \mathbf{u}' \rangle - \langle \mathbf{b}' \mathbf{b}' \rangle)), \end{aligned} \quad (2.5a)$$

$$\frac{\partial \langle \mathbf{B} \rangle}{\partial t} = \nabla \times (\langle \mathbf{U} \rangle \times \langle \mathbf{B} \rangle) + \nabla \times \langle \mathbf{u}' \times \mathbf{b}' \rangle + \eta \nabla^2 \langle \mathbf{B} \rangle, \quad (2.5b)$$

$$\nabla \cdot \langle \mathbf{B} \rangle = 0, \quad \nabla \cdot \langle \mathbf{U} \rangle = 0, \quad (2.5c)$$

where

$$\mathcal{E} = \langle \mathbf{u}' \times \mathbf{b}' \rangle \quad (2.6)$$

is the large-scale EMF and

$$\begin{aligned} \frac{\partial \mathbf{u}'}{\partial t} - \nu \nabla^2 \mathbf{u}' + 2\boldsymbol{\Omega} \times \mathbf{u}' + ((\langle \mathbf{U} \rangle \cdot \nabla) \mathbf{u}' + (\mathbf{u}' \cdot \nabla) \langle \mathbf{U} \rangle - ((\langle \mathbf{B} \rangle \cdot \nabla) \mathbf{b}' - (\mathbf{b}' \cdot \nabla) \langle \mathbf{B} \rangle \\ + \nabla \Pi') = -\nabla \cdot (\mathbf{u}' \mathbf{u}' - \mathbf{b}' \mathbf{b}') + \nabla \cdot (\langle \mathbf{u}' \mathbf{u}' \rangle - \langle \mathbf{b}' \mathbf{b}' \rangle), \end{aligned} \quad (2.7a)$$

$$\begin{aligned} \frac{\partial \mathbf{b}'}{\partial t} - \eta \nabla^2 \mathbf{b}' + ((\langle \mathbf{U} \rangle \cdot \nabla) \mathbf{b}' - ((\langle \mathbf{B} \rangle \cdot \nabla) \mathbf{u}' + (\mathbf{u}' \cdot \nabla) \langle \mathbf{B} \rangle - (\mathbf{b}' \cdot \nabla) \langle \mathbf{U} \rangle \\ = \nabla \times (\mathbf{u}' \times \mathbf{b}' - \langle \mathbf{u}' \times \mathbf{b}' \rangle), \end{aligned} \quad (2.7b)$$

$$\nabla \cdot \mathbf{b}' = 0, \quad \nabla \cdot \mathbf{u}' = 0. \quad (2.7c)$$

3. Non-equilibrium effects in dynamo theory

The non-equilibrium effect in turbulent transport is ubiquitously seen in systems with inhomogeneous boundaries such as a temperature difference, chemical-potential difference, velocity shear, etc. In such non-equilibrium systems, fluxes of energy and matter are sustained by inhomogeneous boundaries or external forcing. If the transport coefficients themselves nonlinearly depend on the inhomogeneous boundaries of the system, the deviation from the equilibrium state can be enhanced. The non-equilibrium properties of turbulence are sometimes represented by a memory effect on the transport coefficient (Hubbard & Brandenburg 2009). The memory effect based on the response function or time integral kernel gives further information on the turbulent transport beyond the simple argument based on the moments of correlation functions.

In the TSDIA formulation, we express the turbulent fluxes with the aid of a derivative expansion and the response functions as well as the correlation functions of the turbulence fields. The response functions provide information as to how much the state of the past and remote points affects the present state. In this sense, the TSDIA provides a straightforward framework for investigating the non-equilibrium effect coupling with large-scale inhomogeneities and external fields in turbulence transport. In order to completely investigate a complicatedly coupled system of field equations, we have to consider the cross-interaction responses among the coupled field quantities as well as the self-interaction responses. In the compressible hydrodynamic turbulence analysis, the cross-interaction responses among the density, momentum and internal energy or temperature fields should be taken into account. In a similar way, in the solenoidal MHD case, the cross-interaction responses between the velocity and magnetic field fluctuations should be considered.

Depending on the level of the non-equilibrium properties of turbulence, which is determined by the inhomogeneous boundaries and external force to the system, the magnitude of the cross-interaction response diversely changes. By assuming some symmetry or anti-symmetry of the correlation functions, response functions and external forcing, we delve into the conditions for and properties of the non-equilibrium effect on the dynamo-related transports.

3.1. Implementation of the TSDIA

Previous results of Mizerski (2018a,b, 2020, 2021a, 2022), obtained in the absence of the Coriolis force but with chiral stochastic forcing, in the context of the geodynamo and galactic dynamos, suggest that the non-stationary α -effect is proportional to the energy production rate resulting from the presence of the forcing (e.g. stochastic buoyancy) and is oscillatory on time scales induced by the forcing, which could be long (see also Mizerski, Bajer & Moffatt (2012) for non-stationary dynamo in the context of the elliptical instability). Here we utilise the TSDIA in order to extract the effect of non-stirred, non-equilibrium turbulence on the large-scale hydromagnetic dynamo. In other words, the new approach allows us to study non-stationary MHD turbulence and the turbulent dynamo effect in the absence of external stochastic forcing although with assumed statistical properties of the background turbulence. We demonstrate that in non-equilibrium turbulence the quantity $\langle \mathbf{u}' \cdot \mathbf{j}' \rangle$ plays a significant role in the generation of the large-scale EMF through the α -effect and the effect of $\langle \mathbf{u}' \cdot \mathbf{j}' \rangle$ vanishes in stationary turbulence.

The validity of the TSDIA formulation can be examined by comparing the theoretical results for turbulent fluxes with experimental or observational measurements and

numerical results. For example, in hydrodynamic turbulence with mean shear flow, the eddy-viscosity representation of the Reynolds stress has been established for several flow geometries. With the TSDIA formulation, we can obtain the eddy-viscosity representation and its departures with a proper evaluation of the model constant (Yoshizawa 1984). In more complex configurations with rotation and/or a magnetic field, we obtain some additional terms arising from the rotation, mean vorticity and magnetic field. For instance, one of the additional terms related to the rotation and mean vorticity, which are coupled with the inhomogeneous turbulent helicity, provides a good agreement with the spatial distribution of the Reynolds stress obtained by the direct numerical simulations of rotating turbulence with an imposed non-uniform distribution of the turbulent helicity by a forcing (Yokoi & Brandenburg 2016). Good agreement is also obtained for the turbulent EMF expression in the Kolmogorov flow configuration with an imposed magnetic field in the dynamo context (Yokoi & Balarac 2011).

3.2. Application of the TSDIA method

Let us introduce a small parameter δ and define slow and fast spatial and temporal variables:

$$\xi = x, \quad X = \delta x, \quad \tau = t, \quad T = \delta t. \quad (3.1a-d)$$

The smallness of δ ensures the presence of scale separation. The large-scale fields depend only on the slow variables $\langle U \rangle(X, T)$ and the fluctuations depend on both, $u'(\xi, X; \tau, T)$. We also define the Fourier transform, involving Galilean transformation to the frame moving with velocity $\langle U \rangle$:

$$u'_i(\xi, X; \tau, T) = \int d^3k \hat{u}'_i(k, X; \tau, T) \exp(-ik \cdot (\xi - \langle U \rangle \tau)), \quad (3.2)$$

but the explicit dependence on the slow variables X and T will be typically suppressed in notation for clarity. The details of the TSDIA approach are provided in Appendix A (see also § 9.6 of Yoshizawa 1998 and Yoshizawa 1985, 1990; Yokoi 2023b) and here we present the major results. The method involves introduction of the concept of background turbulence with given statistical properties, uninfluenced by the large-scale field and rotation, hence isotropic; this background turbulence is defined by the following correlation functions:

$$\langle \hat{f}_i(k; \tau) \hat{g}_j(k_1; \tau_1) \rangle = \left[P_{ij}(k) Q_{fg}(k; \tau, \tau_1) + \frac{1}{2} i \epsilon_{ijk} \frac{k_k}{k^2} H_{fg}(k; \tau, \tau_1) \right] \delta(k + k_1), \quad (3.3)$$

$$\langle G'_{fgij}(k; \tau, \tau_1) \rangle = P_{ij}(k) G_{fg}(k; \tau, \tau_1), \quad (3.4)$$

where f and g represent one of the variables u'_{00} and b'_{00} and $G'_{fgij}(k; \tau, \tau_1)$ denote the Green's functions describing the system's response to infinitesimal disturbances; $P_{ij}(k)$ is a projection operator on the plane perpendicular to the wavevector k . It is useful at this stage to write down explicitly the following quantity:

$$\begin{aligned} \langle u'_{00}(x, \tau) \cdot j'_{00}(x, \tau_1) \rangle &= -i \epsilon_{ijk} \int dk \int dk' k'_j \langle \hat{u}'_{00i}(k; \tau) \hat{b}'_{00k}(k'; \tau_1) \rangle \exp(-i(k + k') \cdot x) \\ &= \int dk H_{ub}(k; \tau, \tau_1) = \int dk H_{bu}(k; \tau_1, \tau), \end{aligned} \quad (3.5)$$

since this quantity will play an important role in the theory of the non-equilibrium α -effect, developed below.

The derivation of the formula for the EMF presented in [Appendix A](#) leads to

$$\mathcal{E} = \alpha \langle \mathbf{B} \rangle - (\beta + \zeta) \langle \mathbf{J} \rangle - \nabla \zeta \times \langle \mathbf{B} \rangle + \gamma (\langle \mathbf{W} \rangle + 2\Omega), \quad (3.6)$$

where $\mathbf{J} = \nabla \times \mathbf{B} = \langle \mathbf{J} \rangle + \mathbf{j}'$ and $\mathbf{W} = \nabla \times \mathbf{U} = \langle \mathbf{W} \rangle + \mathbf{w}'$ denote electric currents and the vorticity respectively. The statistically stationary case has been studied in detail in Yoshizawa (1998) and Yokoi (2013, 2018). When δ is not small, higher-order derivatives in space and time may play important roles in (3.6). See § 7.2 of Brandenburg & Chen (2020) for an example. See also Appendix A.4 of Yokoi (2013) regarding the assumptions and limitations of the TSDIA.

In previous papers on the non-equilibrium dynamo effect, such as Mizerski (2021a, 2022), turbulence is driven by a Gaussian forcing with correlations varying slowly in time. Mizerski (2018a) considered the effect of beating waves, leading to weak non-stationarity, which effectively is very similar to the forcing formulation. Since the total turbulence fields treated in the TSDIA formulation are not at all homogeneous isotropic turbulence but inhomogeneous and anisotropic, this method suits treating non-stationarity (inhomogeneity in time). Examples of investigations of the non-stationarity or non-equilibrium properties of turbulence within the TSDIA can be seen, for example, in Yoshizawa & Nisizima (1993) for homogeneous shear flow turbulence and Yokoi, Masada & Takiwaki (2022) and Yokoi (2023a) for the non-equilibrium effect associated with plume motions in stellar convection.

We now concentrate on the α -effect, which can be decomposed into two contributions,

$$\alpha = \alpha_S + \alpha_X, \quad (3.7)$$

the standard one, related to the so-called residual helicity

$$\begin{aligned} \alpha_S = & \frac{1}{3} \int d^3k \int_{-\infty}^{\tau} d\tau_1 [G_{uu}(k, X; \tau, \tau_1, T) H_{bb}(k, X; \tau, \tau_1, T) \\ & - G_{bb}(k, X; \tau, \tau_1, T) H_{uu}(k, X; \tau_1, \tau, T)], \end{aligned} \quad (3.8)$$

and a less obvious one, related to the cross-helicity and the quantity $\langle \mathbf{u}' \cdot \mathbf{j}' \rangle$ which takes the form

$$\begin{aligned} \alpha_X = & -\frac{1}{3} \int d^3k \int_{-\infty}^{\tau} d\tau_1 G_{bu}(k, X; \tau, \tau_1, T) H_{ub}(k, X; \tau, \tau_1, T) \\ & + \frac{1}{3} \int d^3k \int_{-\infty}^{\tau} d\tau_1 G_{ub}(k, X; \tau, \tau_1, T) H_{bu}(k, X; \tau, \tau_1, T). \end{aligned} \quad (3.9)$$

Since the helical functions of the background turbulence satisfy

$$H_{bu}(\tau, \tau_1) = H_{ub}(\tau_1, \tau), \quad (3.10)$$

we obtain

$$\begin{aligned} \alpha_X = & -\frac{1}{3} \int d^3k \int_{-\infty}^{\tau} d\tau_1 G_{bu}(k, X; \tau, \tau_1, T) H_{ub}(k, X; \tau, \tau_1, T) \\ & + \frac{1}{3} \int d^3k \int_{-\infty}^{\tau} d\tau_1 G_{ub}(k, X; \tau, \tau_1, T) H_{ub}(k, X; \tau_1, \tau, T). \end{aligned} \quad (3.11)$$

We now introduce the following symmetric and anti-symmetric parts of H_{ub} with respect to exchange of time variables:

$$H_{ub}^{(s)}(\tau, \tau_1) = \frac{1}{2}(H_{ub}(\tau, \tau_1) + H_{ub}(\tau_1, \tau)), \quad (3.12a)$$

$$H_{ub}^{(a)}(\tau, \tau_1) = \frac{1}{2}(H_{ub}(\tau, \tau_1) - H_{ub}(\tau_1, \tau)), \quad (3.12b)$$

which allows us to further separate the α_X term into two contributions:

$$\begin{aligned} \alpha_X = & -\frac{1}{3} \int d^3k \int_{-\infty}^{\tau} d\tau_1 [G_{ub}(k, X; \tau, \tau_1, T) + G_{bu}(k, X; \tau, \tau_1, T)] H_{ub}^{(a)}(k, X; \tau, \tau_1, T) \\ & + \frac{1}{3} \int d^3k \int_{-\infty}^{\tau} d\tau_1 [G_{ub}(k, X; \tau, \tau_1, T) - G_{bu}(k, X; \tau, \tau_1, T)] H_{ub}^{(s)}(k, X; \tau_1, \tau, T). \end{aligned} \quad (3.13)$$

The first term in (3.13), i.e.

$$\begin{aligned} \alpha_{\text{neq}} = & -\frac{1}{3} \int d^3k \int_{-\infty}^{\tau} d\tau_1 [G_{ub}(k, X; \tau, \tau_1, T) \\ & + G_{bu}(k, X; \tau, \tau_1, T)] H_{ub}^{(a)}(k, X; \tau, \tau_1, T), \end{aligned} \quad (3.14)$$

clearly constitutes a contribution from non-stationarity of the turbulence, as the anti-symmetric part $H_{ub}^{(a)}$ is clearly a non-equilibrium effect.

3.3. Physics of the non-equilibrium α_{neq} -effect

The α_{neq} -effect originates from the cross-interaction responses between the velocity and magnetic field fluctuations. The importance of the cross-interaction response effects in turbulent transport depends on how and how much the relevant statistical quantities are present in turbulence. There are certain conditions for the α_{neq} -effect to work. The first one is the coupling of the velocity response to the magnetic disturbance, and the counterpart of the magnetic field to the velocity disturbance. This is related to the cross-correlation between the velocity and magnetic field fluctuations: the presence of turbulent cross-helicity ($\langle \mathbf{u}' \cdot \mathbf{b}' \rangle \neq 0$). Another is the presence of the torsional correlation represented by the correlation between the velocity fluctuation \mathbf{u}' and the electric current density fluctuation \mathbf{j}' ($\langle \mathbf{u}' \cdot \mathbf{j}' \rangle \neq 0$). Since the torsional correlation $\langle \mathbf{u}' \cdot \mathbf{j}' \rangle$ can be considered as some combination of $\langle \mathbf{u}' \cdot \mathbf{b}' \rangle$ and $\langle \mathbf{b}' \cdot \mathbf{j}' \rangle$ or $\langle \mathbf{u}' \cdot \mathbf{w}' \rangle$, the coexistence of the cross-helicity and the kinetic helicity is an indispensable condition. In addition, the non-equilibrium property of turbulence represented by the difference between $H_{ub}(\tau, \tau_1)$ and $H_{ub}(\tau_1, \tau)$ in (3.12b) is an essential ingredient for this effect. These points are further discussed in the rest of this subsection.

If we further assume that the function

$$\mathcal{G}(\tau, \tau_1) = G_{ub}(\tau, \tau_1) + G_{bu}(\tau, \tau_1) \quad (3.15)$$

is independent of k , the non-equilibrium α -effect can be expressed as follows:

$$\alpha_{\text{neq}} = -\frac{1}{3} \int_{-\infty}^{\tau} d\tau_1 \mathcal{G}(\tau, \tau_1) \langle \mathbf{u}'_{00} \cdot \mathbf{j}'_{00} \rangle^{(a)}(\mathbf{x}, \tau, \tau_1), \quad (3.16)$$

where

$$\langle \mathbf{u}'_{00} \cdot \mathbf{j}'_{00} \rangle^{(a)}(\mathbf{x}, \tau, \tau_1) = \frac{1}{2} [\langle \mathbf{u}'_{00}(\mathbf{x}, \tau) \cdot \mathbf{j}'_{00}(\mathbf{x}, \tau_1) \rangle - \langle \mathbf{u}'_{00}(\mathbf{x}, \tau_1) \cdot \mathbf{j}'_{00}(\mathbf{x}, \tau) \rangle]. \quad (3.17)$$

Here, the memory effect, expressed by the time integral in (3.16), is clearly crucial, as $\langle \mathbf{u}'_{00} \cdot \mathbf{j}'_{00} \rangle^{(a)}(\mathbf{x}, \tau, \tau) = 0$. Next, inspection of the evolution equations for the Green's functions leads to the conclusion that G_{ub} must be an odd function of \mathbf{b}'_{00} . This is expected, since the α_X contribution to the α -effect results from the action of the Lorentz force, and since H_{ub} is associated with the quantity $\langle \mathbf{u}'_{00} \cdot \mathbf{j}'_{00} \rangle$, i.e. H_{ub} is linear in \mathbf{b}'_{00} , it follows that G_{ub} must be an odd function of the latter. Moreover, since $\langle \mathbf{u}'_{00} \cdot \mathbf{j}'_{00} \rangle$ is a pure scalar quantity (which does not change sign under reflection), G_{ub} must be a pseudoscalar. The only dynamical quantity that is a pseudoscalar and odd in \mathbf{b}'_{00} is the cross-helicity, $\langle \mathbf{u}'_{00} \cdot \mathbf{b}'_{00} \rangle$; hence we expect that $G_{ub} \propto Q_{ub}$. Having in mind that the response function $\mathcal{G}(\tau, \tau_1)$ is non-dimensional we can now provide the following rough estimate of the non-equilibrium α_{neq} -effect:

$$\alpha_{\text{neq}} \approx -\frac{2}{3} \int_{-\infty}^{\tau} d\tau_1 \Upsilon^{(s)}(\mathbf{x}, \tau, \tau_1) \langle \mathbf{u}'_{00} \cdot \mathbf{j}'_{00} \rangle^{(a)}(\mathbf{x}, \tau, \tau_1), \quad (3.18)$$

where

$$\Upsilon(\mathbf{x}, \tau, \tau_1) = \frac{\langle \mathbf{u}'_{00}(\mathbf{x}, \tau) \cdot \mathbf{b}'_{00}(\mathbf{x}, \tau_1) \rangle}{\sqrt{\langle u'^2_{00} \rangle(\mathbf{x}, \tau) \langle b'^2_{00} \rangle(\mathbf{x}, \tau_1)}}, \quad (3.19)$$

$$\Upsilon^{(s)}(\mathbf{x}, \tau, \tau_1) = \frac{1}{2} [\Upsilon(\mathbf{x}, \tau, \tau_1) + \Upsilon(\mathbf{x}, \tau_1, \tau)], \quad (3.20)$$

and the cross-helicity has been normalised by the geometric mean of the kinetic and magnetic fluctuational energies (see Yokoi (2011) for a discussion of different cross-helicity normalisations). The latter equation expresses an effect which results from the lack of equilibrium in the turbulent state.

The second term in (3.13) is likely to be small because of the factor $G_{ub}(\tau, \tau_1) - G_{bu}(\tau, \tau_1)$. For example in the case when $\nu = \eta$ the two response functions G_{ub} and G_{bu} are equal and $\alpha_X = \alpha_{\text{neq}}$ (see discussion at the end of § A.4 in Appendix A). This still holds approximately true when the diffusivities are unequal but weak (the difference between ν and η is much smaller than their sum):

$$G_{ub} \approx G_{bu}, \quad \text{and} \quad \alpha_X \approx \alpha_{\text{neq}}. \quad (3.21a,b)$$

The same symmetry arguments as in the case of α_{neq} can also be applied to the second term in (3.13) which is proportional to the non-dimensional cross-helicity $\Upsilon = \Upsilon(\mathbf{x}, \tau, \tau)$ and the quantity $\langle \mathbf{u}'_{00} \cdot \mathbf{j}'_{00} \rangle = \langle \mathbf{u}'_{00}(\mathbf{x}, \tau) \cdot \mathbf{j}'_{00}(\mathbf{x}, \tau) \rangle$, i.e. $\alpha_X - \alpha_{\text{neq}} \approx \tau_i \Upsilon \langle \mathbf{u}'_{00} \cdot \mathbf{j}'_{00} \rangle$, where τ_i is the turnover time of the most energetic turbulent eddies. However, as remarked above, this effect should be weak when the diffusion is weak or the magnetic Prandtl number $Pr_M = \nu/\eta \approx 1$.

Finally, we also expect the $\langle \mathbf{u}'_{00} \cdot \mathbf{j}'_{00} \rangle$ correlations in fully turbulent flows to be proportional to the kinetic helicity $\langle \mathbf{u}'_{00} \cdot \mathbf{w}'_{00} \rangle$, since typically the velocities and magnetic fields tend to align in such flows. Again, the prefactor must be a pseudoscalar and odd in \mathbf{b}'_{00} ; therefore we propose

$$\langle \mathbf{u}'_{00} \cdot \mathbf{j}'_{00} \rangle \approx \Upsilon \langle \mathbf{u}'_{00} \cdot \mathbf{w}'_{00} \rangle = \frac{\langle \mathbf{u}'_{00} \cdot \mathbf{b}'_{00} \rangle \langle \mathbf{u}'_{00} \cdot \mathbf{w}'_{00} \rangle}{\sqrt{\langle u'^2_{00} \rangle \langle b'^2_{00} \rangle}}. \quad (3.22)$$

We note that the fact of proportionality between $\langle \mathbf{u}'_{00} \cdot \mathbf{j}'_{00} \rangle$ and the cross-helicity is also confirmed by the first-order-smoothing calculation in Appendix B. Introducing the latter

relation into (3.18) leads to

$$\alpha_{\text{neq}} \approx -\frac{2}{3} \int_{-\infty}^{\tau} d\tau_1 (\Upsilon^{(s)}(\mathbf{x}, \tau, \tau_1))^2 \langle \mathbf{u}'_{00} \cdot \mathbf{w}'_{00} \rangle^{(a)}(\mathbf{x}, \tau, \tau_1), \quad (3.23)$$

which shows that the non-equilibrium α_{neq} -effect relies on coexistence of the kinetic helicity and cross-helicity and their history in MHD turbulence (more precisely, in the case of kinetic helicity, only the anti-symmetric part of the temporal correlations $\langle \mathbf{u}'_{00} \cdot \mathbf{w}'_{00} \rangle^{(a)}(\mathbf{x}, \tau, \tau_1)$ contributes to the new effect).

3.4. Calculation of the α_{neq} -effect

We now investigate this dynamo mechanism in some more detail. In order to calculate the effect of non-equilibrium turbulence, we adopt a similar approach to that in Yoshizawa (1984) (see his equations (B2)–(B4); see also chapter 6 of Yoshizawa (1998)). In stationary turbulence the functions $H_{fg}(k, X; \tau, \tau_1, T)$ and $G_f(k, X; \tau, \tau_1, T)$ depend only on $|\tau - \tau_1|$. Hence to study the non-equilibrium effects we postulate formulae for these functions similar to those of Yoshizawa (1984), but modified in order to introduce simple explicit and distinct dependencies on τ and τ_1 :

$$H_{ub}(k, X; \tau, \tau_1, T) = \sigma(k, X, T) \exp(-\varpi(k, X, T) |\tau - \tau_1|) \mathcal{H}(\tau) \mathcal{H}_1(\tau_1), \quad (3.24)$$

$$G_{ub}(k, X; \tau, \tau_1, T) = \theta(\tau - \tau_1) \varsigma(k, X, T) \exp(-\varpi(k, X, T) |\tau - \tau_1|) \mathcal{G}(\tau) \mathcal{G}_1(\tau_1), \quad (3.25)$$

for some functions $\mathcal{H}(\tau)$, $\mathcal{H}_1(\tau_1)$, $\mathcal{G}(\tau)$ and $\mathcal{G}_1(\tau_1)$. Here, $\sigma(k, X, T)$ is the spectral function of the torsional correlation $\langle \mathbf{u}' \cdot \mathbf{j}' \rangle$, $\varsigma(k, X, T)$ is the counterpart of the cross-interaction response G_{ub} and $\theta(t)$ is the Heaviside unit step function that is $\theta = 1$ and $\theta = 0$ for $t > 0$ and $t < 0$, respectively. This in fact follows a standard type of ansatz used in turbulence modelling starting with Taylor (1921) and Tennekes (1979), which has been utilised in conjunction with the TSDIA approach by Yoshizawa (1984). Here this model is used to show explicitly how non-stationarity generates the α_{neq} -correction and to emphasise the role of the dynamical history of the helicities.

We can decompose these functions, \mathcal{H} , \mathcal{H}_1 , \mathcal{G} and \mathcal{G}_1 , into Fourier modes, which allows us to adopt the following, simpler, generic model:

$$H_{ub}(\tau, \tau_1) = \sigma \exp(-\varpi |\tau - \tau_1|) \sin(\varpi_{h0}\tau) \sin(\varpi_{h1}\tau_1), \quad (3.26a)$$

$$G_{ub}(\tau, \tau_1) = \theta(\tau - \tau_1) \varsigma \exp(-\varpi |\tau - \tau_1|) \sin(\varpi_{g0}\tau) \sin(\varpi_{g1}\tau_1), \quad (3.26b)$$

where the dependence on the slow variables and the wavenumber k was suppressed in notation for clarity; moreover $\varpi > 0$ and to fix ideas we also assume $\varpi_{h0} > 0$, $\varpi_{g0} > 0$, $\varpi_{h1} > 0$ and $\varpi_{g1} > 0$. For the sake of simplicity we also assume

$$G_{ub} \approx G_{bu}. \quad (3.27)$$

The following calculation:

$$\begin{aligned} & \int_{-\infty}^{\tau} d\tau_1 G_{ub}(\tau, \tau_1) H_{ub}(\tau, \tau_1) \\ &= \frac{\sigma \varsigma}{4} (\cos \Delta_0 \tau - \cos \Sigma_0 \tau) \left[\frac{1}{4\varpi^2 + \Delta_1^2} (2\varpi \cos \Delta_1 \tau + \Delta_1 \sin \Delta_1 \tau) \right. \\ & \quad \left. - \frac{1}{4\varpi^2 + \Sigma_1^2} (2\varpi \cos \Sigma_1 \tau + \Sigma_1 \sin \Sigma_1 \tau) \right], \end{aligned} \quad (3.28)$$

where

$$\Delta_i = \varpi_{hi} - \varpi_{gi}, \quad \Sigma_i = \varpi_{hi} + \varpi_{gi}, \quad (3.29a,b)$$

shows that in non-equilibrium turbulence both contributions to the α -effect, the ‘standard’ α_S and that associated with cross-helicity α_X , are enhanced by non-stationarity. Since the frequencies correspond to the fast oscillations of turbulent fluctuations in most of the cases the cosines and sines do not contribute to large time scales (their time average vanishes). Under the time average over long time scales $\delta^{-1}t$ the non-zero contribution comes from the cases $\varpi_{hi} = \varpi_{gi}$ (or $\varpi_{hi} \approx \varpi_{gi}$). Therefore we pick $(\varpi, \varpi_h, \varpi_g)$ modes such that the following relations are satisfied:

$$\Delta_i \ll \varpi \ll \varpi_{hi}, \varpi_{gi}, \quad \text{for } i = 0, 1, \quad (3.30)$$

in which case

$$\int_{-\infty}^{\tau} d\tau_1 G_{ub}(\tau, \tau_1) H_{ub}(\tau, \tau_1) \approx \frac{\sigma \varsigma}{8\varpi}; \quad (3.31)$$

for comparison in the stationary case one obtains $\sigma_s \varsigma_s / 2\varpi_s$ with $H_{ub} = \sigma_s \exp(-\varpi_s |\tau - \tau_1|)$, $G_{ub} = \varsigma_s \exp(-\varpi_s |\tau - \tau_1|)$. However, the influence of non-stationarity on the ‘standard’ α_S contribution has been studied using different methods in Mizerski (2018a,b, 2020, 2021a, 2022); note that the relation (3.30) clearly corresponds to the effect of beating waves inducing non-stationarity in the turbulent wave field, discussed in those works. Here we concentrate on the cross-helicity contribution $\alpha_X \approx \alpha_{neq}$, which is apparent within the TSDIA approach. Introduction of the formulae (3.26a,b) into (3.14) yields

$$\alpha_{neq} \approx -\frac{\pi}{6} \int dk \frac{\sigma \varsigma k^2}{\varpi}. \quad (3.32)$$

According to our previous observations in the above, we have $\varsigma \propto \Upsilon$. We note that a very similar result is obtained if one assumes a simpler non-stationary form of the H_{ub} and G_{ub} functions:

$$H_{ub}(\tau, \tau_1) = \sigma \exp(-\varpi |\tau - \tau_1|) \sin [\varpi_h (\tau - \tau_1)], \quad (3.33a)$$

$$G_{ub}(\tau, \tau_1) = \theta(\tau - \tau_1) \varsigma \exp(-\varpi |\tau - \tau_1|) \sin [\varpi_g (\tau - \tau_1)], \quad (3.33b)$$

which satisfies $H_{ub}(\tau, \tau_1) = -H_{ub}(\tau_1, \tau)$, and considers the limit (3.30).

In the above calculation we have used some standard models of the statistical properties of turbulence in order to emphasise the importance of non-stationarity and the history of evolution of the helicities in the turbulent dynamo process. The α_{neq} -effect, induced by the simultaneous presence of cross-helicity and kinetic helicity, can be strong and depends on their magnitude. All the three ingredients are crucial: (i) cross-helicity, (ii) kinetic helicity and (iii) non-stationarity. In turbulence which possesses the cross-helicity and kinetic helicity in abundance and which is out of equilibrium, a correction to the standard α -effect is created, which involves the cross-helicity and memory effects. Such effects can be most straightforwardly treated by closure theories with response or Green’s function formulation. The TSDIA formulation provides a framework for such an analysis.

4. Coexistence of the kinetic helicity and cross-helicity in turbulence

We now consider the question of the likelihood of coexistence of the cross-helicity and kinetic helicity in developed turbulence. Although it is not possible to draw definite

conclusions in this matter, it is still instructive to study the sources and sinks of the cross-helicity in turbulent flows in order to develop some intuition about its generation.

In Appendix B we consider stirred turbulence (with homogeneous, isotropic, stationary and helical Gaussian forcing) and show that under the first-order smoothing approximation (FOSA) the cross-helicity is proportional to the product $\langle \mathbf{B} \rangle \cdot \boldsymbol{\Omega}$ and hence within the FOSA approach the coexistence of the kinetic helicity and cross-helicity is dependent on the existence of the mean field component parallel to the background rotation vector.

A more general calculation is presented in Appendix C, where we derive the general evolution equation for the cross-helicity (see also Yokoi & Hamba 2007; Yokoi 2011; Yokoi & Balarac 2011; Yokoi & Hoshino 2011; Yokoi 2013). This equation involves mean quantities such as the mean EMF \mathcal{E} and the mean Reynolds and Maxwell stresses $\langle u'_i u'_j - b'_i b'_j \rangle$. For the former we utilise the result (3.6) and for the latter we take the expression obtained also via the TSDIA approach in Yokoi & Hoshino (2011), i.e.

$$-\langle u'_i u'_j - b'_i b'_j \rangle \frac{\partial \langle \mathbf{B} \rangle_i}{\partial x_j} = \frac{7}{10} \beta \mathcal{S}_{ij} \mathcal{M}_{ij} - \frac{7}{10} \gamma \text{Tr}(\mathcal{M}^2), \quad (4.1)$$

where

$$\mathcal{S}_{ij} = \frac{\partial \langle \mathbf{U} \rangle_i}{\partial x_j} + \frac{\partial \langle \mathbf{U} \rangle_j}{\partial x_i}, \quad \mathcal{M}_{ij} = \frac{\partial \langle \mathbf{B} \rangle_i}{\partial x_j} + \frac{\partial \langle \mathbf{B} \rangle_j}{\partial x_i}. \quad (4.2a,b)$$

This leads to

$$\begin{aligned} \frac{D}{Dt} \langle \mathbf{u}' \cdot \mathbf{b}' \rangle &= -\alpha (\langle \mathbf{B} \rangle \cdot \langle \mathbf{W} \rangle + 2 \langle \mathbf{B} \rangle \cdot \boldsymbol{\Omega}) + (\beta + \zeta) (\langle \mathbf{J} \rangle \cdot \langle \mathbf{W} \rangle + 2 \langle \mathbf{J} \rangle \cdot \boldsymbol{\Omega}) \\ &\quad - \gamma (\langle \mathbf{W} \rangle + 2 \boldsymbol{\Omega})^2 - \frac{7}{10} \gamma \text{Tr}(\mathcal{M}^2) \\ &\quad + \frac{7}{10} \beta \text{Tr}(\mathcal{S} \cdot \mathcal{M}) + (\nabla \zeta \times \langle \mathbf{B} \rangle) \cdot (\langle \mathbf{W} \rangle + 2 \boldsymbol{\Omega}) \\ &\quad + \nabla \cdot \left[\left(-\Pi' + \frac{\mathbf{u}'^2 + \mathbf{b}'^2}{2} \right) \mathbf{b}' \right] \\ &\quad + \left(\frac{\mathbf{u}'^2 + \mathbf{b}'^2}{2} \right) \langle \mathbf{B} \rangle - \nu \langle \mathbf{w}' \times \mathbf{b}' \rangle + \eta \langle \mathbf{u}' \times \mathbf{j}' \rangle \\ &\quad - (\nu + \eta) \langle \mathbf{w}' \cdot \mathbf{j}' \rangle. \end{aligned} \quad (4.3)$$

Of course if the turbulence is stirred with some forcing \mathbf{f} there is also another production term $\langle \mathbf{f} \cdot \mathbf{b}' \rangle$.

According to (3.23) the magnitude of the non-equilibrium α -effect depends on both the kinetic helicity and cross-helicity and their history. The total α -effect consists of the two contributions $\alpha = \alpha_S + \alpha_X$, where the standard one can be assumed proportional to the kinetic helicity, $\alpha_S \approx -\tau_t \langle \mathbf{u}' \cdot \mathbf{w}' \rangle / 3$. The final balance between the two contributions α_S and α_X determines whether the α coefficient has the same or the opposite sign to the kinetic helicity. The effect of different terms in (4.3) has been studied in the aforementioned works of Yokoi & Hamba (2007), Yokoi (2011), Yokoi & Balarac (2011), Yokoi & Hoshino (2011) and Yokoi (2013) under some simplifying assumptions, in particular under the neglect of the effects from the G_{ub} and G_{bu} response functions, responsible for the non-equilibrium effects studied here. Assuming that $\alpha = -\tau_t \langle \mathbf{u}' \cdot \mathbf{w}' \rangle / 3$, they showed that the first term $-\alpha \langle \mathbf{B} \rangle \cdot \langle \mathbf{W} \rangle$ always leads to destruction of the cross-helicity. This is no longer true when $\gamma \neq 0$ in non-equilibrium turbulence, since depending on the balance between the α_S and

	$\frac{g}{c_s^2 k_1}$	$\frac{v_{A0}}{c_s}$	$\frac{\langle \mathbf{u}' \cdot \mathbf{b}' \rangle}{\sqrt{\langle u'^2 \rangle \langle b'^2 \rangle}}$	$\frac{\langle \mathbf{u}' \cdot \mathbf{w}' \rangle}{\sqrt{\langle u'^2 \rangle \langle w'^2 \rangle}}$	$\frac{\langle \mathbf{b}' \cdot \mathbf{j}' \rangle}{\sqrt{\langle u'^2 \rangle \langle w'^2 \rangle}}$	$\frac{\alpha_{\text{neq}}}{\alpha_0}$	$\frac{\alpha_S}{\alpha_0}$	$\frac{u_{\text{rms}}}{c_s}$	$\frac{v_A^{\text{rms}}}{c_s}$
C	0.5	0.01	-9.8×10^{-3}	-1.6×10^{-2}	-2.0×10^{-4}	7.8×10^{-4}	1.8×10^{-2}	0.10	0.03
A	1.0	0.01	-1.7×10^{-2}	-3.0×10^{-2}	-3.3×10^{-4}	1.1×10^{-3}	3.5×10^{-2}	0.11	0.04
D	2.0	0.01	-2.0×10^{-2}	-3.6×10^{-2}	-2.8×10^{-4}	6.1×10^{-4}	4.1×10^{-2}	0.16	0.04
E	0.5	0.10	-5.5×10^{-2}	-1.9×10^{-2}	-6.2×10^{-4}	-5.6×10^{-3}	1.5×10^{-2}	0.08	0.07
B	1.0	0.10	-5.3×10^{-2}	-3.2×10^{-2}	-1.2×10^{-2}	2.3×10^{-3}	1.8×10^{-2}	0.09	0.12

TABLE 1. Summary of the simulation results for Runs A–E.

α_X terms the term $-\alpha \langle \mathbf{B} \rangle \cdot \langle \mathbf{W} \rangle$ in (4.3) may either amplify or destroy the cross-helicity. Furthermore, Yokoi & Hoshino (2011) take $\beta + \zeta \propto \langle u'^2 \rangle$ and $\gamma \propto \langle \mathbf{u}' \cdot \mathbf{b}' \rangle$ which allows them to identify another two terms that always lead to destruction of the cross-helicity, namely

$$-\gamma (\langle \mathbf{W} \rangle + 2\Omega)^2 - \frac{7}{10}\gamma \text{Tr}(\mathcal{M}^2). \quad (4.4)$$

In addition Yokoi & Hoshino (2011) have described various situations when the terms $(\beta + \zeta) \langle \mathbf{J} \rangle \cdot \langle \mathbf{W} \rangle$, $\beta \text{Tr}(\mathcal{S} \cdot \mathcal{M})$ and $\nabla \cdot [\langle \mathbf{u}^2 + \mathbf{b}^2 \rangle \langle \mathbf{B} \rangle]$ may lead to production of the cross-helicity in the geometry of tokamak devices. Finally, in the term $-2\alpha \langle \mathbf{B} \rangle \cdot \Omega$ we recover the action of the mean field component parallel to the rotation vector, as in the FOSA approach.

The action of all the other terms in (4.3) is difficult to predict and, in general, they can either amplify or destroy the cross-helicity in developed turbulence. The final balance on the right-hand side of (4.3) depends on many dynamical features of turbulence and is expected to be time-dependent. Therefore in order to demonstrate the possibility of coexistence of the cross-helicity and kinetic helicity in magnetised turbulence we have performed numerical simulations of the compressible version of (2.1a–c) in the presence of gravity, density stratification and an imposed magnetic field $\mathbf{g} \parallel \nabla \rho \parallel \mathbf{B}_0 \parallel \Omega$ in a periodic box with the use of the PENCIL CODE (Pencil Code Collaboration *et al.* 2021) with 256^3 mesh points; stress-free and perfectly conducting boundary conditions were imposed at the top and bottom boundaries (see Appendix D). The action of rotation along the direction of stratification leads to kinetic helicity (see figure 5 of Jabbari *et al.* (2014) for simulation results) and the action of a magnetic field along the direction of stratification leads to cross-helicity (Rüdiger, Kitchatinov & Brandenburg 2011).

The values of the physical parameters are as follows. Working again with the unscaled magnetic field $B = 0.01 c_s \sqrt{\mu_0 \bar{\rho}}$ and gravity $g = 1 c_s^2 k_1$ (these are varied in other runs), where c_s is the speed of sound, $\Omega = 0.5 c_s k_1$ is kept fixed in all runs, $\bar{\rho}$ is the mean density and k_1 is the box wavenumber; the remaining parameters, which are constant for all runs are listed in table 1, where we used the Alfvén speed $v_A = B / \sqrt{\mu_0 \bar{\rho}}$ to quantify the strength of the imposed and root-mean-square magnetic fields through v_{A0} and v_A^{rms} , respectively. The results obtained for two values of the imposed magnetic field which differ by an order of magnitude at variable gravity strength are depicted in figure 1 and tables 1 and 2; see also Appendix E for additional figures. The normalised helicities $\langle \mathbf{u}' \cdot \mathbf{b}' \rangle / \sqrt{\langle u'^2 \rangle \langle b'^2 \rangle}$ and $\langle \mathbf{u}' \cdot \mathbf{w}' \rangle / \sqrt{\langle u'^2 \rangle \langle w'^2 \rangle}$ are plotted against time and they are both clearly non-zero in all the considered cases; the cross-helicity is plotted in red and the blue lines correspond to the kinetic helicity whereas their time averages are marked with white lines. In addition, only for the sake of reference, the figures also show the estimates

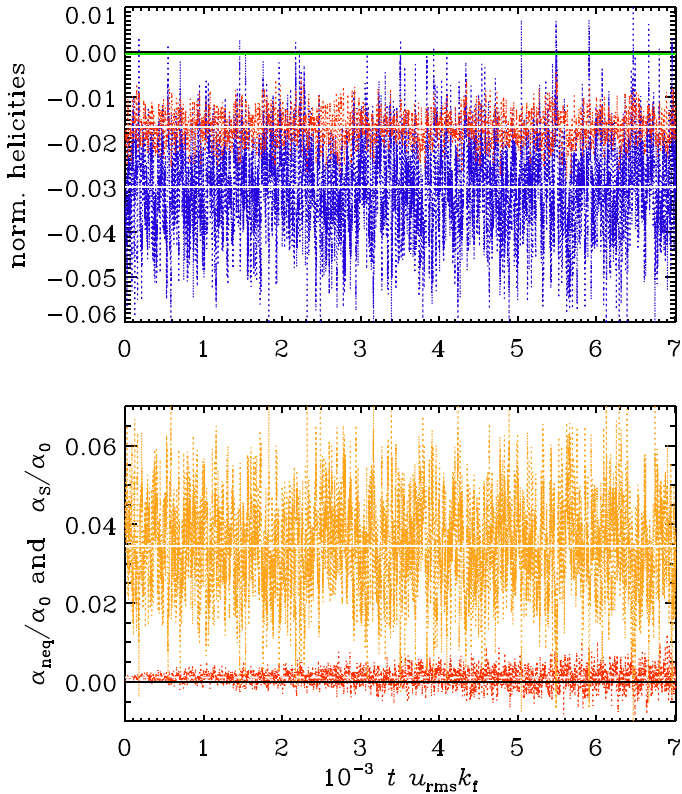


FIGURE 1. Results for Run A of numerical simulations of MHD turbulence in a periodic box with the use of the PENCIL CODE. The upper panel shows the time evolution of the normalised cross-helicity $\langle \mathbf{u}' \cdot \mathbf{b}' \rangle / \sqrt{\langle u'^2 \rangle \langle b'^2 \rangle}$ (red) and the kinetic helicity $\langle \mathbf{u}' \cdot \mathbf{w}' \rangle / \sqrt{\langle u'^2 \rangle \langle w'^2 \rangle}$ (blue); the time averages are marked with the white continuous lines and the green line depicts the current helicity $\langle \mathbf{b}' \cdot \mathbf{j}' \rangle / \sqrt{\langle u'^2 \rangle \langle w'^2 \rangle}$. The estimates of the coefficients α_{neq} (4.5) and α_S (4.6) as functions of time (normalised with $\alpha_0 = u_{\text{rms}}/3$) are provided in the bottom panel in red and orange respectively; the continuous white line marks the time-averaged value of α_S/α_0 and the dashed white line the time average of $\alpha_{\text{neq}}/\alpha_0$.

of the non-equilibrium effect in the form

$$\alpha_{\text{neq}} \approx -\frac{1}{3} \frac{\langle \mathbf{u}' \cdot \mathbf{b}' \rangle}{\sqrt{\langle u'^2 \rangle \langle b'^2 \rangle}} \int_{-\infty}^{\tau} d\tau_1 [\langle \mathbf{u}'(\mathbf{x}, \tau) \cdot \mathbf{j}'(\mathbf{x}, \tau_1) \rangle - \langle \mathbf{u}'(\mathbf{x}, \tau_1) \cdot \mathbf{j}'(\mathbf{x}, \tau) \rangle], \quad (4.5)$$

which can be compared with the following standard estimate of the α -effect, associated with the presence of the kinetic and current helicities:

$$\alpha_S \approx -\frac{1}{3} \tau_t (\langle \mathbf{u}' \cdot \mathbf{w}' \rangle - \langle \mathbf{b}' \cdot \mathbf{j}' \rangle), \quad (4.6)$$

where $\tau_t = 1/(u_{\text{rms}} k_f)$ is the turnover time of the most energetic turbulent eddies, with $u_{\text{rms}} = \sqrt{\langle u'^2 \rangle}$ and $k_f = 30k_1$ denoting the wavenumber of the energy-carrying eddies, which is here the wavenumber of the forcing, and $k_1 = 2\pi/L$ is the lowest wavenumber of the domain of length L .

Although in the numerically studied cases the statistical non-stationarity of turbulence is rather weak and the estimate of the α_{neq} coefficient is always at least an order of magnitude

	k_f	$\frac{\langle \mathbf{u}' \cdot \mathbf{b}' \rangle}{\sqrt{\langle u'^2 \rangle \langle b'^2 \rangle}}$	$\frac{\langle \mathbf{u}' \cdot \mathbf{w}' \rangle}{\sqrt{\langle u'^2 \rangle \langle w'^2 \rangle}}$	$\frac{\langle \mathbf{b}' \cdot \mathbf{j}' \rangle}{\sqrt{\langle u'^2 \rangle \langle w'^2 \rangle}}$	$\frac{\alpha_{\text{neq}}}{\alpha_0}$	$\frac{\alpha_S}{\alpha_0}$	$\frac{u_{\text{rms}}}{c_s}$	$\frac{v_A^{\text{rms}}}{c_s}$
A	30	-1.7×10^{-2}	-3.0×10^{-2}	-3.3×10^{-4}	1.1×10^{-3}	3.5×10^{-2}	0.11	0.04
A2	10	-1.3×10^{-1}	-1.2×10^{-1}	1.3×10^{-3}	-1.7×10^{-2}	6.9×10^{-2}	0.12	0.12
A3	3	-6.4×10^{-2}	-2.1×10^{-1}	-3.0×10^{-2}	-6.0×10^{-3}	5.5×10^{-2}	0.19	0.09

TABLE 2. Summary of the simulation results for Runs A, A2 and A3.

weaker than α_S , the former is clearly different from zero and its relative importance seems to correlate with the magnitude of the cross-helicity. The relative enhancement of the α_{neq} -effect visible for a stronger magnetic field (Run B) and weaker gravity (Run E) corresponds to the enhancement of the cross-helicity with respect to the kinetic helicity. Of course in the latter case (see figure 2), although the α_{neq} coefficient has the largest relative magnitude, it also has a different sign from α_S , hence in this case the non-equilibrium effects tend to suppress the standard dynamo effect. In figure 3 we see that weak magnetic field and strong gravity have suppressed the non-equilibrium effect to a very small relative magnitude.

At smaller scale separation, i.e. for smaller values of k_f , we expect the turbulence to be more intermittent and the degree of non-stationarity to be enhanced. To address this possibility, we have performed additional simulations for smaller values of k_f with the other parameters being the same as for Run A. The results shown in table 2 do show that α_{neq} is twice as large when k_f is reduced from 30 to 10, but an additional decrease of k_f from 10 to 3 does not lead to an additional increase of α_{neq} . To some extent, however, this is caused by the normalisation by α_0 , which has increased by about 60 %.

We conclude that in fully developed helical turbulence, that is, in turbulence with strong kinetic helicity, the cross-helicity is rather likely to be produced as well and at least for some periods of time the two helicities can coexist. Through direct numerical simulation, we confirmed that the non-equilibrium effect derived by the TSDIA formulation did indeed alter the α -effect.

5. Conclusions

We have analysed the hydromagnetic dynamo process in non-equilibrium turbulence. It was shown that in non-equilibrium MHD turbulence the effect of the infinitesimal-impulse cross responses $\mathbf{u}' \leftrightarrow \mathbf{b}'$ is pronounced, which vanishes in the stationary state. This creates additional terms in the expression for the large-scale EMF.

The main conclusion is that the non-equilibrium effects in MHD turbulence modify the α -effect by introducing a correction dependent on the square of the non-dimensional cross-helicity $\Upsilon = \langle \mathbf{u}' \cdot \mathbf{b}' \rangle / \sqrt{\langle u'^2 \rangle \langle b'^2 \rangle}$, the kinetic helicity and their history in the MHD turbulence, which takes the form provided in (3.23). This requires coexistence of both the kinetic helicity and cross-helicity in the turbulent flow. The discussion of the production mechanisms of the cross-helicity, provided in § 4, and the results of numerical simulations lead to the conclusion that such coexistence is possible and perhaps even ubiquitous in many natural systems. Simple strong production mechanisms have been identified already and thoroughly discussed in earlier works (e.g. Yokoi & Hoshino 2011).

The non-equilibrium effects in turbulence affect also other components of the mean EMF in (3.6), that is, the turbulent diffusivity β and the coefficients ζ and γ , in a

non-trivial way, through the effect of the Green's cross-response functions G_{ub} and G_{bu} . This interesting topic should be investigated in more detail in future studies.

Acknowledgements

We are indebted to the two reviewers for their useful suggestions. We would like to thank the Isaac Newton Institute for Mathematical Sciences, Cambridge, for support and hospitality during the programme 'Frontiers in dynamo theory: from the Earth to the stars' (DYT2) where much of the work on this paper was undertaken. Some part of this work was done during N.Y.'s stay at the Nordic Institute for Theoretical Physics (NORDITA) for the programme 'Towards a comprehensive model of the galactic magnetic field' held during 3–28 April 2023.

Editor Steve Tobias thanks the referees for their advice in evaluating this article.

Funding

K.A.M. was supported by a subsidy from the Polish Ministry of Education and Science for the Institute of Geophysics, Polish Academy of Sciences. N.Y. was supported by the Japan Society of the Promotion of Science (JSPS) Grants-in-Aid for Scientific Research JP18H01212 and JP23H01199. We also acknowledge the support of EPSRC grant no. EP/R014604/1 and the Swedish Research Council (Vetenskapsrådet, 2019-04234). Nordita is sponsored by Nordforsk. We acknowledge the allocation of computing resources provided by the Swedish National Allocations Committee at the Center for Parallel Computers at the Royal Institute of Technology in Stockholm and Linköping.

Declaration of interests

The authors report no conflict of interest.

Data availability statement

The data that support the findings of this study are openly available on Zenodo at doi: [10.5281/zenodo.7683615](https://doi.org/10.5281/zenodo.7683615) (v2023.02.28). All calculations have been performed with the PENCIL CODE: doi:[10.5281/zenodo.3961647](https://doi.org/10.5281/zenodo.3961647).

Appendix A. Outline of the TSDIA with self- and cross-interaction response functions for the velocity and magnetic fields

The TSDIA is a combination of the direct-interaction approximation (DIA) for strongly nonlinear homogeneous isotropic turbulence and the multiple-scale analysis with the derivative expansion with respect to the large-scale inhomogeneity. The TSDIA provides a powerful tool for investigating strongly nonlinear turbulence with large-scale inhomogeneities. In applying the TSDIA scheme to MHD, the Elsässer variable formulation has been often adopted. In this formulation, symmetries of the velocity and magnetic field equations are fully utilised, which reduces the complexities in treating the original MHD equations. The correspondence between the Elsässer variable formulation and the usual velocity–magnetic field formulation in the TSDIA has been discussed in some literature (Yoshizawa 1998; Hamba & Sato 2008; Yokoi 2013). Here, we present the outline of the TSDIA formulation under the velocity and magnetic field variables with special reference to the self- and cross-interaction response functions in MHD turbulence (see also Yokoi 2023b). For the outline of the DIA in the context of the TSDIA, the reader is referred to textbooks such as Yoshizawa (1998) and Yokoi (2020).

A.1. Wavenumber space equations

We introduce the Fourier representation concerning the fast space variable ξ as

$$f'(\xi, X; \tau, T) = \int dk f(k, X; \tau, T) \exp[-ik \cdot (\xi - \langle U \rangle \tau)], \quad (\text{A1})$$

where the Fourier transform of the fast variable is taken in the frame co-moving with the local mean velocity $\langle U \rangle$. Hereafter, for the sake of simplicity of notation, the arguments of the slow variable for the fluctuation field $f(\xi, X; \tau, T)$ are suppressed and just denoted as $f(\xi; \tau)$.

The system of two-scale differential equations under the velocity and magnetic field variables in the wavenumber space is written as

$$\begin{aligned} & \frac{\partial u^i(k; \tau)}{\partial \tau} + \nu k^2 u^i(k; \tau) + ik^j \langle B \rangle^j b^i(k; \tau) \\ & - iM^{ij\ell}(k) \iint dp dq \delta(k - p - q) \times [u^j(p; \tau) u^\ell(q; \tau) - b^j(p; \tau) b^\ell(q; \tau)] \\ & = \delta \left[-P^{ij}(k) \frac{\hat{D}u^j(k; \tau)}{DT_I} - P^{ij}(k) u^m(k; \tau) \left(\frac{\partial \langle U \rangle^j}{\partial X^m} + \epsilon^{mj\ell} \Omega_0^\ell \right) \right. \\ & \left. + \langle B \rangle^j \frac{\partial b^i(k; \tau)}{\partial X_I^j} + P^{ij}(k) b^m(k; \tau) \frac{\partial \langle B \rangle^j}{\partial X^m} \right], \end{aligned} \quad (\text{A2})$$

$$-ik^j u^j(k; \tau) + \delta \frac{\partial u^j(k; \tau)}{\partial X_I^j} = 0, \quad (\text{A3})$$

$$\begin{aligned} & \frac{\partial b^i(k; \tau)}{\partial \tau} + \eta k^2 b^i(k; \tau) + ik^j \langle B \rangle^j u^i(k; \tau) \\ & + iN^{ij\ell}(k) \iint dp dq \delta(k - p - q) \times [b^j(p; \tau) u^\ell(q; \tau) - u^j(p; \tau) b^\ell(q; \tau)] \\ & = \delta \left[-P^{ij}(k) \frac{\hat{D}b^j(k; \tau)}{DT_I} + P^{ij}(k) b^m(k; \tau) \left(\frac{\partial \langle U \rangle^j}{\partial X^m} + \epsilon^{mj\ell} \Omega_0^\ell \right) \right. \\ & \left. + \langle B \rangle^j \frac{\partial u^i(k; \tau)}{\partial X_I^j} - P^{ij}(k) u^m(k; \tau) \frac{\partial \langle B \rangle^j}{\partial X^m} \right], \end{aligned} \quad (\text{A4})$$

$$-ik^j b^j(k; \tau) + \delta \frac{\partial b^j(k; \tau)}{\partial X_I^j} = 0, \quad (\text{A5})$$

where \hat{D}/DT is defined below, and

$$\left(\nabla_{X_I}, \frac{D}{DT_I} \right) = \exp(-ik \cdot U\tau) \left(\nabla_X, \frac{D}{DT} \right) \exp(ik \cdot U\tau) \quad (\text{A6})$$

is the differential operators in the interaction representation. Here in (A2) and (A4),

$$M^{ijk}(k) = \frac{1}{2} (k^j P^{ik}(k) + k^k P^{ij}(k)), \quad (\text{A7})$$

with the solenoidal projection operator

$$P^{ij}(\mathbf{k}) = \delta^{ij} - \frac{k^i k^j}{k^2} \quad (\text{A8})$$

and

$$N^{ijk}(\mathbf{k}) = \frac{1}{2} (k^j \delta^{ik} - k^k \delta^{ij}). \quad (\text{A9})$$

The operators M and N are point vertices showing the wavenumber conservation among the nonlinear mode coupling with $\delta(\mathbf{k} - \mathbf{p} - \mathbf{q})$.

In (A2) and (A4), in order to keep the material derivatives objective (invariant with respect to transformations between the inertial frame of reference and the frame rotating with angular velocity $\boldsymbol{\Omega}$), we adopt the co-rotational derivative

$$\hat{\frac{D u'^i}{D T}} = \frac{\partial u'^i}{\partial T} + \langle U \rangle^j \frac{\partial u'^i}{\partial X^j} + \epsilon^{jik} \Omega_0^k u'^j \quad (\text{A10})$$

with

$$\boldsymbol{\Omega}_0 = \boldsymbol{\Omega}/\delta \quad (\text{A11})$$

in place of the Lagrange or advective derivative

$$\frac{D u'^i}{D T} = \frac{\partial u'^i}{\partial t} + \langle U \rangle^j \frac{\partial u'^i}{\partial x^j}, \quad (\text{A12})$$

which is not objective with respect to rotation.

A.2. Scale-parameter expansion

Utilising (A3) and (A5) in order to split the dynamical fields into components along the wavevector \mathbf{k} and perpendicular to it, we expand the fields $f(\mathbf{k}; \tau)$ with respect to the scale parameter δ , and then further each of the expansion terms is expanded with respect to the weak mean magnetic field as

$$\begin{aligned} f^i(\mathbf{k}; \tau) &= \sum_{n=0}^{\infty} \delta^n f_n^i(\mathbf{k}; \tau) - \sum_{n=0}^{\infty} \delta^{n+1} i \frac{k^i}{k^2} \frac{\partial}{\partial X_I^j} f_n^j(\mathbf{k}; \tau) \\ &= \sum_{n=0}^{\infty} \sum_{m=0}^{\infty} \delta^n f_{nm}^i(\mathbf{k}; \tau) - \sum_{n=0}^{\infty} \sum_{m=0}^{\infty} \delta^{n+1} i \frac{k^i}{k^2} \frac{\partial}{\partial X_I^j} f_{nm}^j(\mathbf{k}; \tau), \end{aligned} \quad (\text{A13})$$

where the subscript m corresponds to an expansion in the weak mean field. In this two-scale formulation, inhomogeneities and anisotropies enter at the order of the scale parameter δ (with the index n) and the mean field $\langle \mathbf{B} \rangle$ (with the index m). The lowest-order fields f_{00} correspond to homogeneous and isotropic turbulence.

Using the expansion (A13), we write the equations of each order in matrix form. With the abbreviated form of the spectral integral

$$\int_{\Delta} = \iint dp dq \delta(\mathbf{k} - \mathbf{p} - \mathbf{q}), \quad (\text{A14})$$

the $f_{00}(\mathbf{k}; \tau)$ equations are given as

$$\begin{aligned} \begin{pmatrix} 0 \\ 0 \end{pmatrix} &= \begin{pmatrix} \frac{\partial}{\partial \tau} + \nu k^2 & 0 \\ 0 & \frac{\partial}{\partial \tau} + \eta k^2 \end{pmatrix} \begin{pmatrix} u_{00}^i(\mathbf{k}; \tau) \\ b_{00}^i(\mathbf{k}; \tau) \end{pmatrix} \\ &+ i \begin{pmatrix} -M^{ij\ell}(\mathbf{k}) \int_{\Delta} u_{00}^j(\mathbf{p}; \tau) & M^{ij\ell}(\mathbf{k}) \int_{\Delta} b_{00}^j(\mathbf{p}; \tau) \\ N^{ij\ell}(\mathbf{k}) \int_{\Delta} b_{00}^j(\mathbf{p}; \tau) & -N^{ij\ell}(\mathbf{k}) \int_{\Delta} u_{00}^j(\mathbf{p}; \tau) \end{pmatrix} \begin{pmatrix} u_{00}^{\ell}(\mathbf{q}; \tau) \\ b_{00}^{\ell}(\mathbf{q}; \tau) \end{pmatrix}, \end{aligned} \quad (\text{A15})$$

the $f_{01}(\mathbf{k}; \tau)$ equations are given as

$$\begin{aligned} \begin{pmatrix} \frac{\partial}{\partial \tau} + \nu k^2 & 0 \\ 0 & \frac{\partial}{\partial \tau} + \eta k^2 \end{pmatrix} \begin{pmatrix} u_{01}^i(\mathbf{k}; \tau) \\ b_{01}^i(\mathbf{k}; \tau) \end{pmatrix} \\ + i \begin{pmatrix} -2M^{ij\ell}(\mathbf{k}) \int_{\Delta} u_{00}^j(\mathbf{p}; \tau) & 2M^{ij\ell}(\mathbf{k}) \int_{\Delta} b_{00}^j(\mathbf{p}; \tau) \\ 2N^{ij\ell}(\mathbf{k}) \int_{\Delta} b_{00}^j(\mathbf{p}; \tau) & -2N^{ij\ell}(\mathbf{k}) \int_{\Delta} u_{00}^j(\mathbf{p}; \tau) \end{pmatrix} \begin{pmatrix} u_{01}^{\ell}(\mathbf{q}; \tau) \\ b_{01}^{\ell}(\mathbf{q}; \tau) \end{pmatrix} \\ = -ik^j \langle B \rangle^j \begin{pmatrix} 0 & 1 \\ 1 & 0 \end{pmatrix} \begin{pmatrix} u_{00}^i(\mathbf{k}; \tau) \\ b_{00}^i(\mathbf{k}; \tau) \end{pmatrix} \equiv \begin{pmatrix} F_{01u}^i \\ F_{01b}^i \end{pmatrix} \end{aligned} \quad (\text{A16})$$

and the $f_{10}(\mathbf{k}; \tau)$ equations are

$$\begin{aligned} \begin{pmatrix} \frac{\partial}{\partial \tau} + \nu k^2 & 0 \\ 0 & \frac{\partial}{\partial \tau} + \eta k^2 \end{pmatrix} \begin{pmatrix} u_{10}^i(\mathbf{k}; \tau) \\ b_{10}^i(\mathbf{k}; \tau) \end{pmatrix} \\ + i \begin{pmatrix} -2M^{ij\ell}(\mathbf{k}) \int_{\Delta} u_{00}^j(\mathbf{p}; \tau) & 2M^{ij\ell}(\mathbf{k}) \int_{\Delta} b_{00}^j(\mathbf{p}; \tau) \\ 2N^{ij\ell}(\mathbf{k}) \int_{\Delta} b_{00}^j(\mathbf{p}; \tau) & -2N^{ij\ell}(\mathbf{k}) \int_{\Delta} u_{00}^j(\mathbf{p}; \tau) \end{pmatrix} \begin{pmatrix} u_{10}^{\ell}(\mathbf{q}; \tau) \\ b_{10}^{\ell}(\mathbf{q}; \tau) \end{pmatrix} \\ = \langle B \rangle^j \frac{\partial}{\partial X_I^j} \begin{pmatrix} 0 & 1 \\ 1 & 0 \end{pmatrix} \begin{pmatrix} u_{00}^i(\mathbf{k}) \\ b_{00}^i(\mathbf{k}) \end{pmatrix} - P^{ij}(\mathbf{k}) \frac{\hat{D}}{DT_I} \begin{pmatrix} 1 & 0 \\ 0 & 1 \end{pmatrix} \begin{pmatrix} u_{00}^j(\mathbf{k}) \\ b_{00}^j(\mathbf{k}) \end{pmatrix} \end{aligned}$$

$$\begin{aligned}
& + \begin{pmatrix} -P^{ij}(\mathbf{k}) \left(\frac{\partial \langle U \rangle^j}{\partial X^\ell} + \epsilon^{\ell j n} \Omega_0^n \right) & P^{ij}(\mathbf{k}) \frac{\partial \langle B \rangle^j}{\partial X^\ell} \\ -P^{ij}(\mathbf{k}) \frac{\partial \langle B \rangle^j}{\partial X^\ell} & P^{ij}(\mathbf{k}) \left(\frac{\partial \langle U \rangle^j}{\partial X^\ell} + \epsilon^{\ell j n} \Omega_0^n \right) \end{pmatrix} \begin{pmatrix} u_{00}^\ell(\mathbf{k}; \tau) \\ b_{00}^\ell(\mathbf{k}; \tau) \end{pmatrix} \\
& \equiv \begin{pmatrix} F_{10u}^i \\ F_{10b}^i \end{pmatrix}, \tag{A17}
\end{aligned}$$

where F_{01u} , F_{01b} , F_{10u} and F_{10b} denote each component of the second right-hand sides of (A16) and (A17). They can be regarded as the forcing for the evolution equations of $f_{01}(\mathbf{k}; \tau)$ and $f_{10}(\mathbf{k}; \tau)$, respectively.

A.3. Introduction of Green's functions

For the purpose of solving these differential equations, we introduce the Green's functions associated with (A15). We consider the response of the turbulence to an infinitesimal disturbance. Reflecting the structure of the MHD equations and the field expansion (A13), the left-hand side of the linearised differential equations for the Green's function is in the same form as the left-hand sides of (A16) and (A17) or the differential operators to the $f_{01}(\mathbf{k}; \tau)$ and $f_{10}(\mathbf{k}; \tau)$ fields. In order to treat mutual interaction between the velocity and magnetic field, we consider four Green's functions: the Green's function G_{uu} representing the response of the velocity field \mathbf{u} to the velocity perturbation \mathbf{u} ; G_{ub} , the response of \mathbf{u} to the magnetic perturbation \mathbf{b} ; G_{bu} , the response of \mathbf{b} to the velocity perturbation \mathbf{u} ; and G_{bb} , the response of magnetic field \mathbf{b} to the magnetic perturbation \mathbf{b} . From the left-hand sides of (A16) and (A17) we construct the system of equations representing the responses to the infinitesimal forcing. It follows that these four Green's functions should be defined by their evolution equations as

$$\begin{aligned}
& \begin{pmatrix} \frac{\partial}{\partial \tau} + \nu k^2 & 0 \\ 0 & \frac{\partial}{\partial \tau} + \eta k^2 \end{pmatrix} \begin{pmatrix} G_{uu}^{ij} & G_{ub}^{ij} \\ G_{bu}^{ij} & G_{bb}^{ij} \end{pmatrix} \\
& + i \begin{pmatrix} -2M^{ikm} \int_\Delta u_{00}^k & 2M^{ikm} \int_\Delta b_{00}^k \\ 2N^{ikm} \int_\Delta b_{00}^k & -2N^{ikm} \int_\Delta u_{00}^k \end{pmatrix} \begin{pmatrix} G_{uu}^{mj} & G_{ub}^{mj} \\ G_{bu}^{mj} & G_{bb}^{mj} \end{pmatrix} = P^{ij} \delta(\tau - \tau') \begin{pmatrix} 1 & 0 \\ 0 & 1 \end{pmatrix}. \tag{A18}
\end{aligned}$$

Considering that the right-hand sides of (A16) and (A17) are the force terms, we formally solve f_{01} and f_{10} fields with the aid of the Green's functions. The f_{01} fields are expressed as

$$\begin{pmatrix} u_{01}^i \\ b_{01}^i \end{pmatrix} = \int_{-\infty}^{\tau} d\tau_1 \begin{pmatrix} G_{uu}^{ij} & G_{ub}^{ij} \\ G_{bu}^{ij} & G_{bb}^{ij} \end{pmatrix} \begin{pmatrix} F_{01u}^j \\ F_{01b}^j \end{pmatrix}. \tag{A19}$$

Note that \mathbf{u}_{01} and \mathbf{b}_{01} are expressed by \mathbf{b}_{00} and \mathbf{u}_{00} coupled with the mean magnetic field $\langle \mathbf{B} \rangle$, respectively. Consequently, \mathbf{u}_{01} and \mathbf{b}_{01} multiplied by \mathbf{b}_{00} and \mathbf{u}_{00} in an external product manner will not contribute to the EMF.

On the other hand, the f_{10} fields are expressed as

$$\begin{pmatrix} u_{10}^i \\ b_{10}^i \end{pmatrix} = \int_{-\infty}^{\tau} d\tau_1 \begin{pmatrix} G_{uu}^{ij} & G_{ub}^{ij} \\ G_{bu}^{ij} & G_{bb}^{ij} \end{pmatrix} \begin{pmatrix} F_{10u}^j \\ F_{10b}^j \end{pmatrix}. \tag{A20}$$

A.4. Statistical assumption on the basic fields

We assume that the basic or lowest-order fields are homogeneous and isotropic:

$$\frac{\langle \vartheta_{00}^i(\mathbf{k}; \tau) \chi_{00}^j(\mathbf{k}'; \tau') \rangle}{\delta(\mathbf{k} + \mathbf{k}')} = P^{ij}(\mathbf{k}) Q_{\vartheta\chi}(\mathbf{k}; \tau, \tau') + \frac{i}{2} \frac{k^\ell}{k^2} \epsilon^{ij\ell} H_{\vartheta\chi}(\mathbf{k}; \tau, \tau'), \quad (\text{A21})$$

where ϑ_{00} and χ_{00} represent one of \mathbf{u}_{00} and \mathbf{b}_{00} , and the indices ϑ and χ represent one of u and b . The Green's functions are written as

$$\langle G_{\vartheta\chi}^{ij}(\mathbf{k}; \tau, \tau') \rangle = P^{ij}(\mathbf{k}) G_{\vartheta\chi}(\mathbf{k}; \tau, \tau'). \quad (\text{A22})$$

The spectral functions Q_{uu} , Q_{bb} , Q_{ub} , H_{uu} , H_{bb} , H_{ub} and H_{bu} are related to the turbulent statistical quantities (the turbulent kinetic energy, magnetic energy, cross-helicity, kinetic helicity, electric current helicity, torsional correlations between velocity and magnetic field) of the basic or lowest-order fields as

$$\int d\mathbf{k} Q_{uu}(k; \tau, \tau) = \langle \mathbf{u}'_{00}^2 \rangle / 2, \quad (\text{A23})$$

$$\int d\mathbf{k} Q_{bb}(k; \tau, \tau) = \langle \mathbf{b}'_{00}^2 \rangle / 2, \quad (\text{A24})$$

$$\int d\mathbf{k} Q_{ub}(k; \tau, \tau) = \langle \mathbf{u}'_{00} \cdot \mathbf{b}'_{00} \rangle, \quad (\text{A25})$$

$$\int d\mathbf{k} H_{uu}(k; \tau, \tau) = \langle \mathbf{u}'_{00} \cdot \mathbf{w}'_{00} \rangle, \quad (\text{A26})$$

$$\int d\mathbf{k} H_{bb}(k; \tau, \tau) = \langle \mathbf{b}'_{00} \cdot \mathbf{j}'_{00} \rangle, \quad (\text{A27})$$

$$\int d\mathbf{k} H_{ub}(k; \tau, \tau) = \langle \mathbf{u}'_{00} \cdot \mathbf{j}'_{00} \rangle, \quad (\text{A28})$$

$$\int d\mathbf{k} H_{bu}(k; \tau, \tau) = \langle \mathbf{b}'_{00} \cdot \mathbf{w}'_{00} \rangle. \quad (\text{A29})$$

Under the renormalisation procedure briefly described below (equation (A31)) and in detail in Yoshizawa (1998), the Green's function can effectively be treated as deterministic: $G_{bu}^{ij}(\mathbf{k}, \tau, \tau') = P^{ij}G_{bu}(\mathbf{k}, \tau, \tau')$ and $G_{uu}^{ij}(\mathbf{k}, \tau, \tau') = P^{ij}G_{uu}(\mathbf{k}, \tau, \tau')$. We note that, when $\nu = \eta$, the system possesses only two distinct Green's functions, because $G_{uu} = G_{bb}$ and $G_{ub} = G_{bu}$. Under the assumptions (A22) this is clear from (A18). Although the operator M^{ijk} differs from N^{ikm} , the contributions from the contraction with $k_m P_{ik}$ vanish for solutions of (A18).

A.5. Calculation of the EMF

The turbulent EMF is expressed in terms of the wavenumber representation of the velocity and magnetic field as

$$E_M^i \equiv \epsilon^{ijk} \langle u^j b'^k \rangle = \epsilon^{ijk} \int d\mathbf{k} \langle u^j(\mathbf{k}; \tau) b^k(\mathbf{k}'; \tau) \rangle / \delta(\mathbf{k} + \mathbf{k}'). \quad (\text{A30})$$

Using the results of (A19) and (A20), we calculate the velocity–magnetic field correlation up to the $f_{01}g_{00}$ and $f_{10}g_{00}$ orders as

$$\langle u^j b^k \rangle = \langle u_{00}^j b_{00}^k \rangle + \langle u_{01}^j b_{00}^k \rangle + \langle u_{00}^j b_{01}^k \rangle + \delta \langle u_{10}^j b_{00}^k \rangle + \delta \langle u_{00}^j b_{10}^k \rangle + \dots. \quad (\text{A31})$$

In the DIA formalism, the lowest-order spectral functions Q_{uu} , Q_{bb} , Q_{ub} , H_{uu} , H_{bb} , H_{ub} and H_{bu} and the lowest-order Green's functions G_{uu} , G_{bb} , G_{ub} and G_{bu} are replaced with their exact counterparts, \tilde{Q}_{uu} , \tilde{Q}_{bb} , ... and \tilde{G}_{uu} , \tilde{G}_{bb} , ..., respectively. Under this renormalisation procedure on the propagators (spectral and response functions), important turbulent correlation functions are calculated. For the sake of simplicity, hereafter, the tilde denoting an exact propagator is omitted as $\tilde{Q}_{uu} \rightarrow Q_{uu}$, $\tilde{G}_{uu} \rightarrow G_{uu}$, etc.

Here we present the final results of the turbulent EMF as

$$\langle \mathbf{u}' \times \mathbf{b}' \rangle = \alpha \langle \mathbf{B} \rangle - (\beta + \zeta) \nabla \times \langle \mathbf{B} \rangle - (\nabla \zeta) \times \langle \mathbf{B} \rangle + \gamma (\langle \mathbf{W} \rangle + 2\Omega), \quad (\text{A32})$$

where transport coefficients α , β , ζ and γ are given as

$$\alpha = \frac{1}{3} [-I\{G_{bb}, H_{uu}\} + I\{G_{uu}, H_{bb}\} - I\{G_{bu}, H_{ub}\} + I\{G_{ub}, H_{bu}\}], \quad (\text{A33})$$

$$\beta = \frac{1}{3} [I\{G_{bb}, Q_{uu}\} + I\{G_{uu}, Q_{bb}\} - I\{G_{bu}, Q_{ub}\} - I\{G_{ub}, Q_{bu}\}], \quad (\text{A34})$$

$$\zeta = \frac{1}{3} [I\{G_{bb}, Q_{uu}\} - I\{G_{uu}, Q_{bb}\} + I\{G_{bu}, Q_{ub}\} - I\{G_{ub}, Q_{bu}\}], \quad (\text{A35})$$

$$\gamma = \frac{1}{3} [I\{G_{bb}, Q_{ub}\} + I\{G_{uu}, Q_{bu}\} - I\{G_{bu}, Q_{uu}\} - I\{G_{ub}, Q_{bb}\}] \quad (\text{A36})$$

with the abbreviated form of integral

$$I\{A, B\} = \int dk \int_{-\infty}^{\tau} d\tau_1 A(k; \tau, \tau_1) B(k; \tau, \tau_1). \quad (\text{A37})$$

Appendix B. Cross-helicity and $\langle \mathbf{u}' \cdot \mathbf{j}' \rangle$ under the FOSA

In the presence of the Coriolis force and under the FOSA, in Fourier space the linearised equations take the form

$$(-i\omega + \nu k^2) \hat{u}_i(\mathbf{q}) + 2\Omega \epsilon_{ijk} \hat{u}_j(\mathbf{q}) = \hat{f}_i(\mathbf{q}) + ik \cdot \langle \mathbf{B} \rangle \hat{b}_i(\mathbf{q}), \quad (\text{B1})$$

$$(-i\omega + \eta k^2) \hat{b}_i(\mathbf{q}) = ik \cdot \langle \mathbf{B} \rangle \hat{u}_i(\mathbf{q}), \quad (\text{B2})$$

where $\mathbf{q} = (\mathbf{k}, \omega)$, the forcing is assumed Gaussian with zero mean, homogeneous, stationary and isotropic,

$$\langle \hat{f}_i(\mathbf{k}, \omega) \hat{f}_j(\mathbf{k}', \omega') \rangle = \left[\frac{D_0}{k^3} P_{ij}(\mathbf{k}) + i \frac{D_1}{k^5} \epsilon_{ijk} k_k \right] \delta(\mathbf{k} + \mathbf{k}') \delta(\omega + \omega'), \quad (\text{B3})$$

and $P_{ij}(\mathbf{k}) = \delta_{ij} - k_i k_j / k^2$ is the projection operator on the plane perpendicular to the wavevector \mathbf{k} . Such type of force correlation is commonly used in the literature (see Landau & Lifshitz 1987) and it was shown by Yakhot & Orszag (1986) and Mizerski (2021b) to correspond to Kolmogorov-type scalings for the spectral turbulent energy and helicity. Introducing

$$\gamma_\nu = -i\omega + \nu k^2, \quad \gamma_\eta = -i\omega + \eta k^2, \quad (\text{B4a,b})$$

and considering the weak seed field limit defined by

$$\langle \mathbf{B} \rangle^2 \ll \langle \mathbf{U} \rangle^2, \quad \text{hence also} \quad \langle \mathbf{b}'^2 \rangle \ll \langle \mathbf{u}'^2 \rangle, \quad (\text{B5})$$

the equations reduce to

$$\hat{u}_i(\mathbf{q}) \approx \mathfrak{G}_{ij} \hat{f}_j(\mathbf{q}), \quad (\text{B6})$$

$$\hat{b}_i(\mathbf{q}) \approx i \frac{\mathbf{k} \cdot \langle \mathbf{B} \rangle}{\gamma_\eta} \mathfrak{G}_{ij} \hat{f}_j(\mathbf{q}), \quad (\text{B7})$$

where

$$\mathfrak{G}_{ij} = \frac{1}{\gamma_v^2 + 4\Omega^2 \frac{k_z^2}{k^2}} \left[\gamma_v \delta_{ij} - 2\Omega \epsilon_{i3j} + 2\Omega \frac{k_i k_m}{k^2} \epsilon_{jm3} \right]. \quad (\text{B8})$$

The cross-helicity takes the form

$$\begin{aligned} \langle h_{ub} \rangle &= \langle u'_i(\mathbf{x}, t) b'_i(\mathbf{x}, t) \rangle \\ &= i \int d^4 q \int d^4 q' \exp(i[(\mathbf{k} + \mathbf{k}') \cdot \mathbf{x} - (\omega + \omega') t]) \\ &\quad \times \frac{\mathbf{k}' \cdot \langle \mathbf{B} \rangle}{\gamma_\eta(\mathbf{q}')} \mathfrak{G}_{ij}(\mathbf{q}) \mathfrak{G}_{ik}(\mathbf{q}') \langle \hat{f}_j(\mathbf{q}) \hat{f}_k(\mathbf{q}') \rangle \\ &= -i \langle B \rangle_m \int d^4 q \frac{k_m}{\gamma_\eta(-\mathbf{q})} \mathfrak{G}_{ij}(\mathbf{q}) \mathfrak{G}_{ik}(-\mathbf{q}) \left[\frac{D_0}{k^3} P_{jk}(\mathbf{k}) + i \frac{D_1}{k^5} \epsilon_{jks} k_s \right] \\ &= -8\Omega \langle B \rangle_m \int_{k_f}^\infty \frac{dk}{k} \int_{-\infty}^\infty d\omega \int_0^{2\pi} d\varphi \int_{-1}^1 dX \frac{\omega^2 D_1}{(\omega^2 + \eta^2 k^4) \mathcal{F}(\omega, X)} \frac{k_z k_m}{k^2} \\ &= -16\pi (\langle \mathbf{B} \rangle \cdot \boldsymbol{\Omega}) \int_{k_f}^\infty \frac{dk}{k} \int_{-\infty}^\infty d\omega \int_{-1}^1 dX \frac{\omega^2 X^2 D_1}{(\omega^2 + \eta^2 k^4) \mathcal{F}(\omega, X)} \\ &= -16\pi D_1 \mathcal{I}(\nu, \eta, \Omega, k_f) (\langle \mathbf{B} \rangle \cdot \boldsymbol{\Omega}), \end{aligned} \quad (\text{B9})$$

where

$$\begin{aligned} \mathcal{F}(\omega, X) &= (\omega^2 + \nu^2 k^4)^2 - 8\Omega^2 X^2 (\omega^2 - \nu^2 k^4) + 16\Omega^4 X^4 \\ &= (\omega^2 - 4\Omega^2 X^2)^2 + 2\omega^2 \nu^2 k^4 + 8\nu^2 k^4 \Omega^2 X^2 + \nu^4 k^8 > 0 \end{aligned} \quad (\text{B10})$$

and

$$\mathcal{I}(\nu, \eta, \Omega, k_f) = \int_{k_f}^\infty \frac{dk}{k} \int_{-\infty}^\infty d\omega \int_{-1}^1 dX \frac{\omega^2 X^2}{(\omega^2 + \eta^2 k^4) \mathcal{F}(\omega, X)} > 0. \quad (\text{B11})$$

On the other hand, for the scalar quantity $\langle s_{uj} \rangle = \langle \mathbf{u}' \cdot \mathbf{j}' \rangle$ this approach yields

$$\begin{aligned} \langle s_{uj} \rangle &= \langle u'_i(\mathbf{x}, t) j'_i(\mathbf{x}, t) \rangle \\ &= -\epsilon_{irt} \langle B \rangle_m \int d^4 q \int d^4 q' \exp(i[(\mathbf{k} + \mathbf{k}') \cdot \mathbf{x} - (\omega + \omega') t]) \\ &\quad \times \frac{k'_r k'_m}{\gamma_\eta(\mathbf{q}')} \mathfrak{G}_{ij}(\mathbf{q}) \mathfrak{G}_{tk}(\mathbf{q}') \langle \hat{f}_j(\mathbf{q}) \hat{f}_k(\mathbf{q}') \rangle \\ &= -\epsilon_{irt} \langle B \rangle_m \int d^4 q \frac{k_r k_m}{\gamma_\eta(-\mathbf{q})} \mathfrak{G}_{ij}(\mathbf{q}) \mathfrak{G}_{ik}(-\mathbf{q}) \left[\frac{D_0}{k^3} P_{jk}(\mathbf{k}) + i \frac{D_1}{k^5} \epsilon_{jks} k_s \right] \\ &= 8\Omega \langle B \rangle_m \int_{k_f}^\infty k dk \int_{-\infty}^\infty d\omega \int_0^{2\pi} d\varphi \int_{-1}^1 dX \frac{\omega^2 D_0}{(\omega^2 + \eta^2 k^4) \mathcal{F}(\omega, X)} \frac{k_z k_m}{k^2} \\ &= 16\pi (\langle \mathbf{B} \rangle \cdot \boldsymbol{\Omega}) \int_{k_f}^\infty k dk \int_{-\infty}^\infty d\omega \int_{-1}^1 dX \frac{\omega^2 X^2 D_0}{(\omega^2 + \eta^2 k^4) \mathcal{F}(\omega, X)} \\ &= 16\pi D_0 \tilde{\mathcal{I}}(\nu, \eta, \Omega, k_f) (\langle \mathbf{B} \rangle \cdot \boldsymbol{\Omega}), \end{aligned} \quad (\text{B12})$$

where

$$\tilde{\mathcal{I}}(\nu, \eta, \Omega, k_f) = \int_{k_f}^{\infty} k dk \int_{-\infty}^{\infty} d\omega \int_{-1}^1 dX \frac{\omega^2 X^2}{(\omega^2 + \eta^2 k^4) \mathcal{F}(\omega, X)} > 0. \quad (\text{B13})$$

In the above we have used

$$\int \frac{k_j}{k'} f(\cos^2 \theta) d\Omega = 0, \quad \int \frac{k_i k_j k_k}{k^3} f(\cos^2 \theta) d\Omega = 0, \quad (\text{B14a,b})$$

$$\int \frac{k_j k_n}{k^2} f(\cos^2 \theta) d\Omega = \pi \int_{-1}^1 f(X^2) \{ \delta_{jn} (1 - X^2) + \delta_{j3} \delta_{n3} (3X^2 - 1) \} dX, \quad (\text{B15})$$

where Ω denotes the solid angle and the spherical coordinates (k, θ, φ) have been used (with a substitution $X = \cos \theta$). We can now utilise the above results to show that

$$\langle \mathbf{u}' \cdot \mathbf{j}' \rangle = - \left(\frac{\tilde{\mathcal{I}}(\nu, \eta, \Omega, k_f) D_0}{\mathcal{I}(\nu, \eta, \Omega, k_f) D_1} \right) \langle \mathbf{u}' \cdot \mathbf{b}' \rangle. \quad (\text{B16})$$

Appendix C. Evolution equations for $\langle \mathbf{u}' \cdot \mathbf{b}' \rangle$ and $\langle \mathbf{u}' \cdot \mathbf{j}' \rangle$

Utilising the evolution equations

$$\begin{aligned} \frac{D\mathbf{u}'}{Dt} = & -\nabla \Pi' - 2\boldsymbol{\Omega} \times \mathbf{u}' - (\mathbf{u}' \cdot \nabla) \langle \mathbf{U} \rangle + (\langle \mathbf{B} \rangle \cdot \nabla) \mathbf{b}' + (\mathbf{b}' \cdot \nabla) \langle \mathbf{B} \rangle + \nu \nabla^2 \mathbf{u}' \\ & + \nabla \cdot (\mathbf{b}' \mathbf{b}') + \nabla \cdot (\langle \mathbf{u}' \mathbf{u}' \rangle - \langle \mathbf{b}' \mathbf{b}' \rangle), \end{aligned} \quad (\text{C1})$$

$$\frac{D\mathbf{b}'}{Dt} = (\langle \mathbf{B} \rangle \cdot \nabla) \mathbf{u}' - (\mathbf{u}' \cdot \nabla) \langle \mathbf{B} \rangle + (\mathbf{b}' \cdot \nabla) \langle \mathbf{U} \rangle + \eta \nabla^2 \mathbf{b}' + (\mathbf{b}' \cdot \nabla) \mathbf{u}' - \nabla \times \boldsymbol{\mathcal{E}}, \quad (\text{C2})$$

where

$$\frac{D}{Dt} = \frac{\partial}{\partial t} + (\langle \mathbf{U} \rangle + \mathbf{u}') \cdot \nabla, \quad (\text{C3})$$

we arrive at

$$\begin{aligned} \frac{D}{Dt} \langle \mathbf{u}' \cdot \mathbf{b}' \rangle = & -\boldsymbol{\mathcal{E}} \cdot ((\mathbf{W}) + 2\boldsymbol{\Omega}) - \langle u'_i u'_j - b'_i b'_j \rangle \partial_j \langle \mathbf{B} \rangle_i \\ & + \nabla \cdot \left[\left\langle \left(-\Pi' + \frac{\mathbf{u}'^2 + \mathbf{b}'^2}{2} \right) \mathbf{b}' \right\rangle + \left\langle \frac{\mathbf{u}'^2 + \mathbf{b}'^2}{2} \right\rangle \langle \mathbf{B} \rangle \right] \\ & - \mu_0 (\nu + \eta) \langle \mathbf{w}' \cdot \mathbf{j}' \rangle \end{aligned} \quad (\text{C4})$$

and

$$\begin{aligned} \frac{D}{Dt} \langle \mathbf{u}' \cdot \mathbf{j}' \rangle = & -\langle \mathbf{u}' \times \mathbf{j}' \rangle \cdot ((\mathbf{W}) + 2\boldsymbol{\Omega}) - \langle w'_i u'_j - j'_i b'_j \rangle \partial_j \langle \mathbf{B} \rangle_i - \partial_j \langle \mathbf{U} \rangle_m \langle \epsilon_{ijk} u'_i \partial_m b'_k \rangle \\ & + \left[(\langle \mathbf{B} \rangle + \mathbf{b}') \cdot \nabla \right] \mathbf{b}' \cdot \mathbf{j}' + \left[(\langle \mathbf{B} \rangle + \mathbf{b}') \cdot \nabla \right] \mathbf{u}' \cdot \mathbf{w}' - u'_i \epsilon_{ijk} \partial_j u'_m \partial_m b'_k \\ & - \nabla \cdot \langle \Pi' \mathbf{j}' \rangle - (\nu - \eta) \langle \mathbf{w}' \cdot \nabla^2 \mathbf{b}' \rangle, \end{aligned} \quad (\text{C5})$$

where in the last equation, apart from no-slip boundary conditions, we have also assumed vanishing of the helical quantity $\langle \mathbf{w}' \cdot \mathbf{j}' \rangle$ at the boundaries.

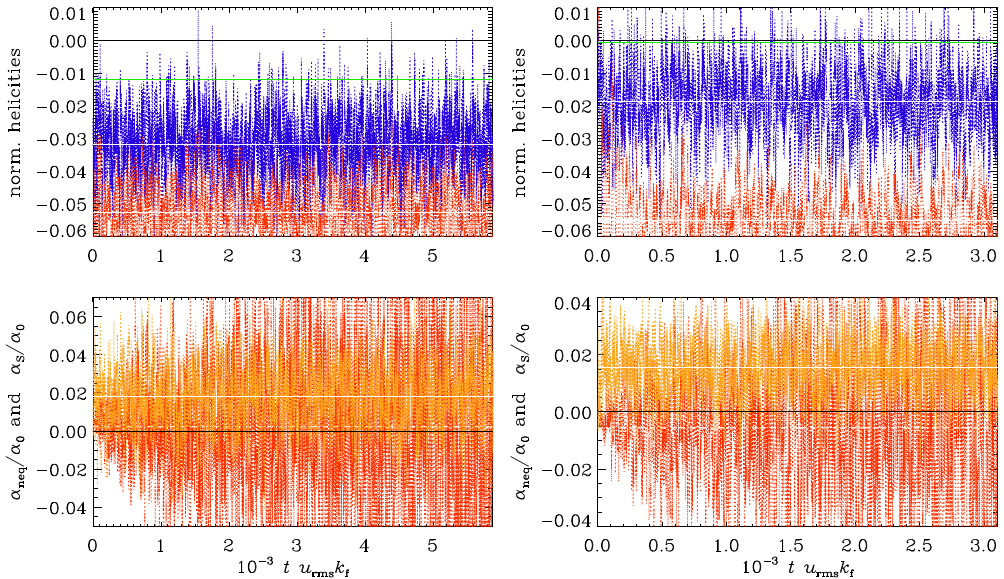


FIGURE 2. Same as figure 1, but for Runs B and E with a stronger magnetic field, $B = 0.1c_s\sqrt{\mu_0\rho}$, and two values of gravity, $g = 1c_s^2k_1$ and $g = 0.5c_s^2k_1$.

Appendix D. Basic equations used in the compressible case

In the numerical simulations, instead of (2.1a–c), we solve the following set of equations for a compressible isothermal gas with constant sound speed c_s for \mathbf{U} , ρ , and the magnetic vector potential \mathbf{A} :

$$\frac{\partial \mathbf{U}}{\partial t} + (\mathbf{U} \cdot \nabla) \mathbf{U} = -c_s^2 \nabla \ln \rho - 2\boldsymbol{\Omega} \times \mathbf{U} + \frac{1}{\rho} \mathbf{J} \times \mathbf{B} - \nu \mathbf{Q} + \mathbf{g} + \mathbf{f}, \quad (\text{D1a})$$

$$\frac{\partial \rho}{\partial t} = -\nabla \cdot (\rho \mathbf{U}), \quad (\text{D1b})$$

$$\frac{\partial \mathbf{A}}{\partial t} = \mathbf{U} \times \mathbf{B} - \eta \mu_0 \mathbf{J}, \quad (\text{D2})$$

where

$$\mathbf{Q} = -\nabla^2 \mathbf{U} - \frac{1}{3} \nabla \nabla \cdot \mathbf{U} - \mathbf{S} \nabla \ln \rho, \quad (\text{D3})$$

$$\mu_0 \mathbf{J} = -\nabla^2 \mathbf{A} + \nabla \nabla \cdot \mathbf{A}, \quad (\text{D4})$$

$$\mathbf{B} = \mathbf{B}_0 + \nabla \times \mathbf{A}, \quad (\text{D5})$$

and

$$\mathbf{S}_{ij} = \frac{1}{2}(\partial_i U_j + \partial_j U_i) - \frac{1}{3}\delta_{ij}\nabla \cdot \mathbf{U} \quad (\text{D6})$$

are the components of the traceless rate-of-strain tensor and \mathbf{f} is a random forcing function consisting of plane unpolarised waves with typical wavenumber k_f and an amplitude such that $u_{\text{rms}}/c_s \approx 0.1$ (see table 1). Here, $\boldsymbol{\Omega} = (0, 0, \Omega)$ is the angular velocity, $\mathbf{g} = (0, 0, -g)$ is gravity, $\mathbf{B}_0 = (0, 0, B_0)$ is the imposed magnetic field, η is the magnetic diffusivity and ν is the kinematic viscosity, whose value is such that $u_{\text{rms}}/\nu k_1 \approx 1000$. A resolution of $N^3 = 256^3$ mesh points is then sufficient. Since we chose $k_f/k_1 = 30$, we

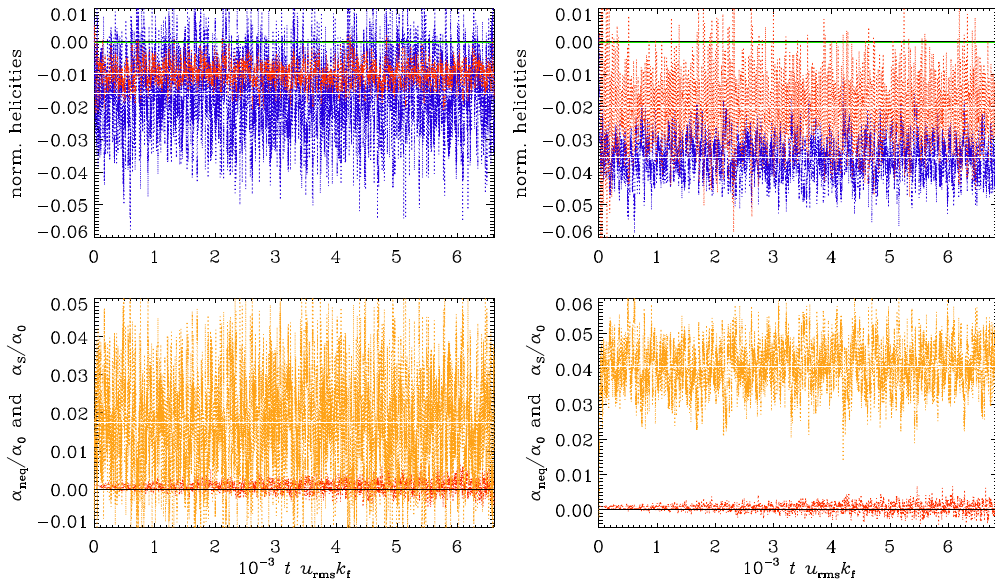


FIGURE 3. Same as figure 1, but for Runs C and D with weaker magnetic field, $B = 0.01c_s\sqrt{\mu_0\bar{\rho}}$, and two values of gravity, $g = 0.5c_s^2k_1$ and $g = 2c_s^2k_1$.

have for the Reynolds number $Re \equiv u_{\text{rms}}/\nu k_f \approx 30$. For the magnetic Prandtl number we chose, as in Jabbari *et al.* (2014), the value $Pr_M \equiv \nu/\eta = 0.5$, so the magnetic Reynolds number is $Re_M \equiv u_{\text{rms}}/\eta k_f \approx 15$. The equilibrium stratification is given by $\ln(\rho/\rho_0) = -z/H_\rho$, where $H_\rho = c_s^2/g$ is the density scale height.

Appendix E. Results for Runs B–E

In figure 2, we present the results for Runs B and E with a stronger magnetic field, $B = 0.1c_s\sqrt{\mu_0\bar{\rho}}$, and two values of gravity, $g = 1c_s^2k_1$ and $g = 0.5c_s^2k_1$. Finally, in figure 3, we present the results for Runs C and D with weaker magnetic field, $B = 0.01c_s\sqrt{\mu_0\bar{\rho}}$, and two values of gravity, $g = 0.5c_s^2k_1$ and $g = 2c_s^2k_1$. In all those cases, we found that $\alpha_{\text{neq}} \neq 0$; see the red lines in the upper panels of figures 2 and 3.

REFERENCES

- BALBUS, S.A. & HAWLEY, J.F. 1991a A powerful local shear instability in weakly magnetized disks. I - Linear analysis. *Astroph. J.* **376**, 214–222.
 BALBUS, S.A. & HAWLEY, J.F. 1991b A powerful local shear instability in weakly magnetized disks. II - Nonlinear evolution. *Astroph. J.* **376**, 223–233.
 BRANDENBURG, A. & CHEN, L. 2020 The nature of mean-field generation in three classes of optimal dynamos. *J. Plasma Phys.* **86**, 905860110.
 BRANDENBURG, A. & SUBRAMANIAN, K. 2005 Astrophysical magnetic fields and nonlinear dynamo theory. *Phys. Rep.* **417**, 1–209.
 DORMY, E. & SOWARD, A.M. 2007 *Mathematical Aspects of Natural Dynamos*. Chapman and Hall/CRC Taylor and Francis Group.
 GIBNEY, E. 2022 Nuclear-fusion reactor smashes energy record. *Nature* **602**, 371.
 HAMBA, F. & SATO, H. 2008 Turbulent transport coefficients and residual energy in mean-field dynamo theory. *Phys. Plasmas* **15**, 022302.
 HAMBA, F. & TSUCHIYA, M. 2010 Cross-helicity dynamo effect in magnetohydrodynamic turbulent channel flow. *Phys. Plasmas* **17**, 012301.

- HUBBARD, A. & BRANDENBURG, A. 2009 Memory effect in turbulence transport. *Astrophys. J.* **706**, 712.
- JABBARI, S., BRANDENBURG, A., LOSADA, I.R., KLEEORIN, N. & ROGACHEVSKII, I. 2014 Magnetic flux concentrations from dynamo-generated fields. *Astron. Astrophys.* **568**, A112.
- KRAUSE, F. & RÄDLER, K.-H. 1980 *Mean-Field Magnetohydrodynamics and Dynamo Theory*. Pergamon Press.
- LANDAU, L.D. & LIFSHITZ, E.M. 1987 *Fluid Mechanics, Course of Theoretical Physics*, vol. 6. Elsevier.
- LI, J., NI, M. & LU, Y. 2019 The frontier and perspective for tokamak development. *Nat. Sci. Rev.* **6** (3), 382–383.
- MIZERSKI, K.A. 2018a Large-scale hydromagnetic dynamo by Lehnert waves in nonresistive plasma. *SIAM J. Appl. Maths* **78**, 1402–1421.
- MIZERSKI, K.A. 2018b Large-scale dynamo action driven by forced beating waves in a highly conducting plasma. *J. Plasma Phys.* **84**, 735840405.
- MIZERSKI, K.A. 2020 Renormalization group analysis of the turbulent hydromagnetic dynamo: the effect of nonstationarity. *Astrophys. J. Suppl.* **251**, 21.
- MIZERSKI, K.A. 2021a Possible role of non-stationarity of magnetohydrodynamic turbulence in understanding of geomagnetic excursions. *Symmetry* **13**, 1881.
- MIZERSKI, K.A. 2021b Renormalization group analysis of the magnetohydrodynamic turbulence and dynamo. *J. Fluid Mech.* **926**, A13.
- MIZERSKI, K.A. 2022 Dynamo effect caused by non-stationary turbulence in strongly magnetized, hot, low-density plasma. *Astron. Astrophys.* **660**, A110.
- MIZERSKI, K.A., BAJER, K. & MOFFATT, H.K. 2012 The mean electromotive force generated by elliptic instability. *J. Fluid Mech.* **707**, 111–128.
- MOFFATT, H.K. & DORMY, E. 2019 *Self-Exciting Fluid Dynamos*. Cambridge University Press.
- PENCIL CODE COLLABORATION, BRANDENBURG, A., JOHANSEN, A., BOURDIN, P.A., DOBLER, W., LYRA, W., RHEINHARDT, M., BINGERT, S., HAUGEN, N.E.L., MEE, A., *et al.* 2021 The Pencil Code, a modular MPI code for partial differential equations and particles: multipurpose and multiuser-maintained. *J. Open Source Softw.* **6**, 2807.
- ROBERTS, P.H. & KING, E.M. 2013 On the genesis of the Earth's magnetism. *Rep. Prog. Phys.* **76**, 096801.
- ROBERTS, P.H. & SOWARD, A.M. 1972 Magnetohydrodynamics of the Earth's core. *Annu. Rev. Fluid Mech.* **4**, 117–154.
- RÜDIGER, G., KITCHATINOV, L.L. & BRANDENBURG, A. 2011 Cross helicity and turbulent magnetic diffusivity in the solar convection zone. *Sol. Phys.* **269**, 3–12.
- TAYLOR, G.I. 1921 Diffusion by continuous movements. *Proc. Lond. Math. Soc.* **20**, 196–212.
- TENNEKES, H. 1979 The exponential Lagrangian correlation function and turbulent diffusion in the inertial subrange. *Atmos. Environ.* **13**, 1565–1567.
- YAKHOT, V. & ORSZAG, S.A. 1986 Renormalization group analysis of turbulence. I. Basic theory. *J. Sci. Comput.* **1**, 3–51.
- YOKOI, N. 2011 Modeling the turbulent cross-helicity evolution: production, dissipation, and transport rates. *J. Turbul.* **12**, N27.
- YOKOI, N. 2013 Cross helicity and related dynamo. *Geophys. Astrophys. Fluid Dyn.* **107**, 114–184.
- YOKOI, N. 2018 Electromotive force in strongly compressible magnetohydrodynamic turbulence. *J. Plasma Phys.* **84**, 735840501.
- YOKOI, N. 2020 Turbulence, transport and reconnection. In *Topics in Magnetohydrodynamic Topology, Reconnection and Stability Theory*, CISM International Centre for Mechanical Sciences 591 (eds. D. MacTaggart & A. Hillier). https://doi.org/10.1007/978-3-030-16343-3_6
- YOKOI, N. 2023a Non-equilibrium turbulent transport in convective plumes obtained from closure theory. *Atmosphere* **14**, 01013.
- YOKOI, N. 2023b Unappreciated cross-helicity effects in plasma physics: anti-diffusion effects in dynamo and momentum transport. *Rev. Mod. Plasma Phys.* (submitted), arXiv:2303.01834.
- YOKOI, N. & BALARAC, G. 2011 Cross-helicity effects and turbulent transport in magnetohydrodynamic flow. *J. Phys.: Conf. Ser.* **318**, 072039.

- YOKOI, N. & BRANDENBURG, A. 2016 Large-scale flow generation by inhomogeneous helicity. *Phys. Rev. E* **93**, 033125.
- YOKOI, N. & HAMBA, F. 2007 An application of the turbulent magnetohydrodynamic residual-energy equation model to the solar wind. *Phys. Plasmas* **14**, 112904.
- YOKOI, N. & HOSHINO, M. 2011 Flow-turbulence interaction in magnetic reconnection. *Phys. Plasmas* **18**, 111208.
- YOKOI, N., MASADA, Y. & TAKIWAKI, T. 2022 Modelling stellar convective transport with plumes – I. Non-equilibrium turbulence effect in double-averaging formulation. *Mon. Not. R. Astron. Soc.* **516**, 2718–2735.
- YOSHIZAWA, A. 1984 Statistical analysis of the deviation of the Reynolds stress from its eddy-viscosity representation. *Phys. Fluids* **27**, 1377–1387.
- YOSHIZAWA, A. 1985 Statistical theory for magnetohydrodynamic turbulent shear flows. *Phys. Fluids* **28**, 3313–3320.
- YOSHIZAWA, A. 1990 Self-consistent turbulent dynamo modeling of reversed field pinches and planetary magnetic fields. *Phys. Fluids B* **2**, 1589–1600.
- YOSHIZAWA, A. 1998 *Hydrodynamic and Magnetohydrodynamic Turbulent Flows: Modelling and Statistical Theory*. Kluwer Academic Publishers.
- YOSHIZAWA, A. & NISIZIMA, S. 1993 A nonequilibrium representation of the turbulent viscosity based on a two-scale turbulence theory. *Phys. Fluids* **5**, 3302–3304.
- ZHOU, H. & BLACKMAN, E.G. 2023 Helical dynamo growth at modest versus extreme magnetic Reynolds numbers. [arXiv:2302.06042](https://arxiv.org/abs/2302.06042).